PilotSTRATEGY

WP2 – Deliverable 2.7 Geological Models Annex (Portugal)

Release Status:
Author: Daniel Marques da Silva, Maria Helena Caeiro, Pedro Pereira, Carlos Ribeiro, Júlio Carneiro, João Casacão, Bruno Pina
Date: July 2023
Filename and Version:
Project ID Number: 101022664

PilotSTRATEGY (H2020- Topic LC-SC3-NZE-6-2020 - RIA)

PilotSTRATEGY

1. Document History

1.1 Location

This document is stored in the following location:

Filename	
Location	

1.2 Revision History

This document has been through the following revisions:

Version No.	Revision Date	Filename/Location stored:	Brief Summary of Changes

1.3 Authorisation

This document requires the following approvals:

AUTHORISATION	Name	Signature	Date
WP Leader	Mark Wilkinson		DD/MM/YY
Project Coordinator	Fernanda de Mesquita Lobo Veloso		DD/MM/YY

For Deliverables, the Project Coordinator should receive the final version at least one week prior to the due date.

1.4 Distribution

document has been distributed to:

Name	Title	Version Issued	Date of Issue
			00/00/0000

The PilotSTRATEGY project has received funding from the European Union's Horizon 2020 research and innovation programme under grant agreement No. 101022664

© European Union, 2023

No third-party textual or artistic material is included in the publication without the copyright holder's prior consent to further dissemination by other third parties.

Reproduction is authorised provided the source is acknowledged.

Disclaimer [to be added to any public deliverables]

The information and views set out in this [report/study/article/publication…] are those of the author(s) and do not necessarily reflect the official opinion of the European Union. Neither the European Union institutions and bodies nor any person acting on their behalf may be held responsible for the use which may be made of the information contained therein.

Table of Contents

The PilotSTRATEGY project has received funding from the European Union's Horizon 2020 research and innovation programme under grant agreement No. 101022664

2. Introduction

This document aims to provide additional information to complete the deliverable 2.7, task 2.3 of work package 2 (WP2, Geocharacterization) of the PilotSTRATEGY Project. Detailed description of the regional geological framework, including sedimentological, structural, and stratigraphical characterization is presented in section 3 – Regional Geological Characterization. The characterization of the storage complex is presented in section 4 – Storage Complex Characterization, and a comprehensive facies analysis of the reservoir and the seal in section 5 – Facies analysis. Section 6 includes the analysis of some outcrops, and in section 7 – Depositional Environments and Geological Conceptual Model, as a conclusion, the main deposition environments of the area of interest and some notes on the conceptual geological model, are stated.

3. Regional Geological Characterization

3.1 Sedimentological and structural context review of the Area of Interest

The study area is located in the offshore domain of the northern sector of the Lusitanian Basin (LB), in western Portugal (Figure 1). LB is a Meso-Cenozoic basin, that evolved as a rift basin throughout most part of the Mesozoic. The basin begins its evolution during the Late Triassic – Early Jurassic with the onset of the first rifting event. Other two rifting events occurred during the Late Jurassic and Early Cretaceous. Continental break-up occurred close to the transition between Early and Late Cretaceous. Mesozoic sedimentation in the LB alternated between deposits with continental influence and marine deposits. Siliciclastic and carbonate sediments are the most common along the basin.

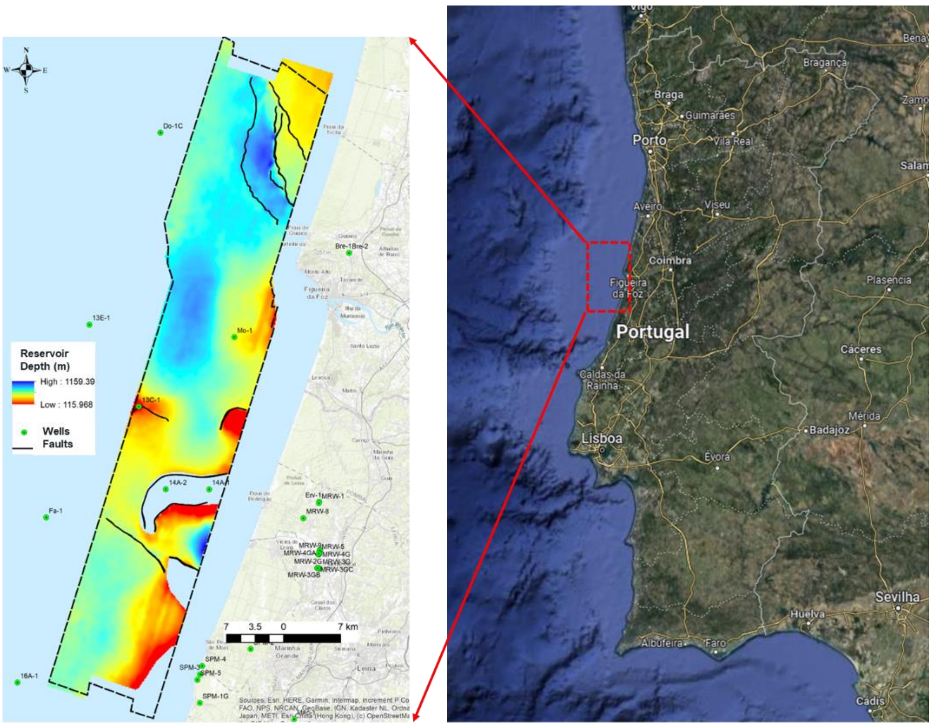

Figure 1: Location of the study area in the offshore of the Portuguese coast (north of Lusitanian Basin). The image shows the depth structural map of Torres Vedras Group (reservoir), interpreted within the 3D seismic volume Cabo Mondego and S. Pedro de Moel, highlighting the main faults in the region.

The PilotSTRATEGY project has received funding from the European Union's Horizon 2020 research and innovation programme under grant agreement No. 101022664

Two potential storage complexes exist at the LB: i) the Triassic-Lower Jurassic Silves Group (reservoir) and Dagorda Formation (seal) and; ii) the Cretaceous Torres Vedras Group (reservoir) and Cacém Formation (seal). New data from PilotSTRATEGY WP2 and re-interpreted data acquired for hydrocarbon exploration dismissed the Triassic-Lower Jurassic storage complex in favour of the Cretaceous one (see deliverable D2.6).

A simplified stratigraphic chart that depicts the tectono-sedimentary packages and the main tectonic events occurring during the Meso-Cenozoic is presented in Figure 2. The LB basin is composed of a series of diapir-bound and fault-bound sub-basins, developed on a horst-graben anisotropic fabric basement controlled by late-Hercynian NNE-SSW and NW-SE strike slip faults, reactivated as normal faults from the onset of the first intracontinental rifting stage during the Late Triassic (Wilson et al., 1989; Pinheiro et al., 1996; Rasmussen et al., 1998). Three (to four) main rifting episodes are recorded in the Lusitanian basin and in the neighbouring Porto basin (Wilson et al., 1989; Pinheiro et al., 1996; Stapel et al., 1996; Leinfelder & Wilson, 1998; Rasmussen et al., 1998; Alves et al., 2003; Alves & Cunha, 2018), which can be defined as: Rift 1a (Late Triassic) and Rift 1b (Early Jurassic), Rift 2 (Late Oxfordian to Berriasian) and Rift 3 (Valanginian/Hauterivian to Aptian, in the continental-slope basins west of the LB).

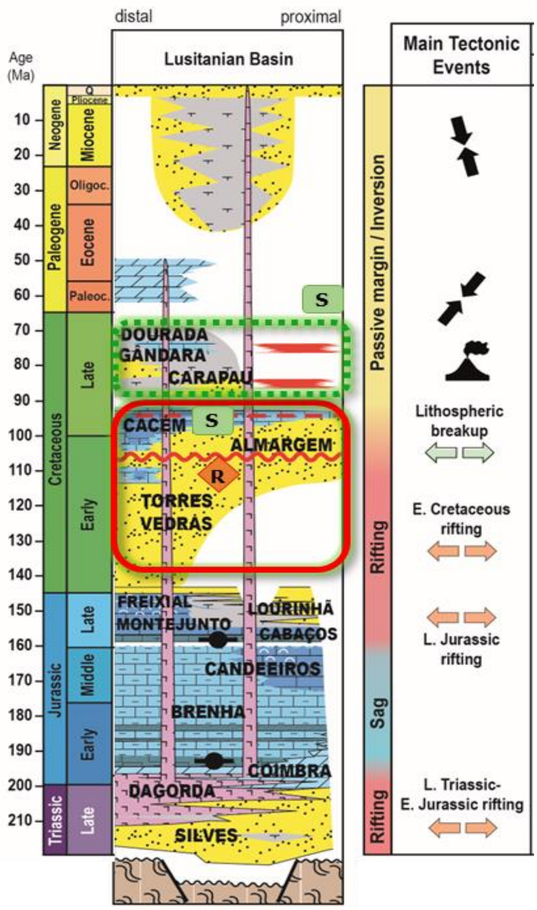

Figure 2: Simplified lithostratigraphic chart of the Lusitanian Basin (adapted from Casacão et al., 2023), including the main tectonic events that impacted the basin's evolution. Here it is highlighted the storage complex play that is being considered, formed by the Torres Vedras Group (reservoir unit) and Cacém Formation (seal), and the secondary seal formed by the Aveiro Group (Carapau, Gândara and Dourada formations).

The PilotSTRATEGY project has received funding from the European Union's Horizon 2020 research and innovation programme under grant agreement No. 101022664

The architecture of LB reflects a continuous syn- to post-rift sedimentary record in a proximal margin with mild subsidence. The geometry and lithostratigraphic record of these packages were largely influenced by normal faulting and salt diapirism throughout the Mesozoic, a major episode of magmatism during the Late Cretaceous and, lastly, a regional-scale tectonic inversion uplift controlled by the Pyrenean (Eocene) and Betic phases (Miocene) of the Alpine orogeny (Terrinha et al., 2019a). This Cenozoic basin inversion resulted in the reactivation of post-Hercynian faults, and in an interplay between thick Hettangian evaporites that were already developed at that time, which caused the reactivation of salt diapirs throughout different compression phases (Ribeiro et al., 1990; Wilson et al., 1989; Pinheiro et al., 1996; Alves et al., 2002).

Various styles of salt diapirism in the onshore Lusitanian Basin (Figure 3) include *the Caldas da Rainha – Óbidos salt wall*; *the Porto de Mós – Rio Maior salt-wall squeezed diapir system*; *buried salt domes* (Wilson et al., 1989); *salt pillows*, whose inflation during the Cenozoic compression phases helped to create the N-verging Boa Viagem thrust system (Ribeiro et al., 1990), close to the study area; and *pop-up occurrences* associated with thin-skinned tectonics during the Miocene (Ribeiro et al., 1990; Kullberg et al., 2013).

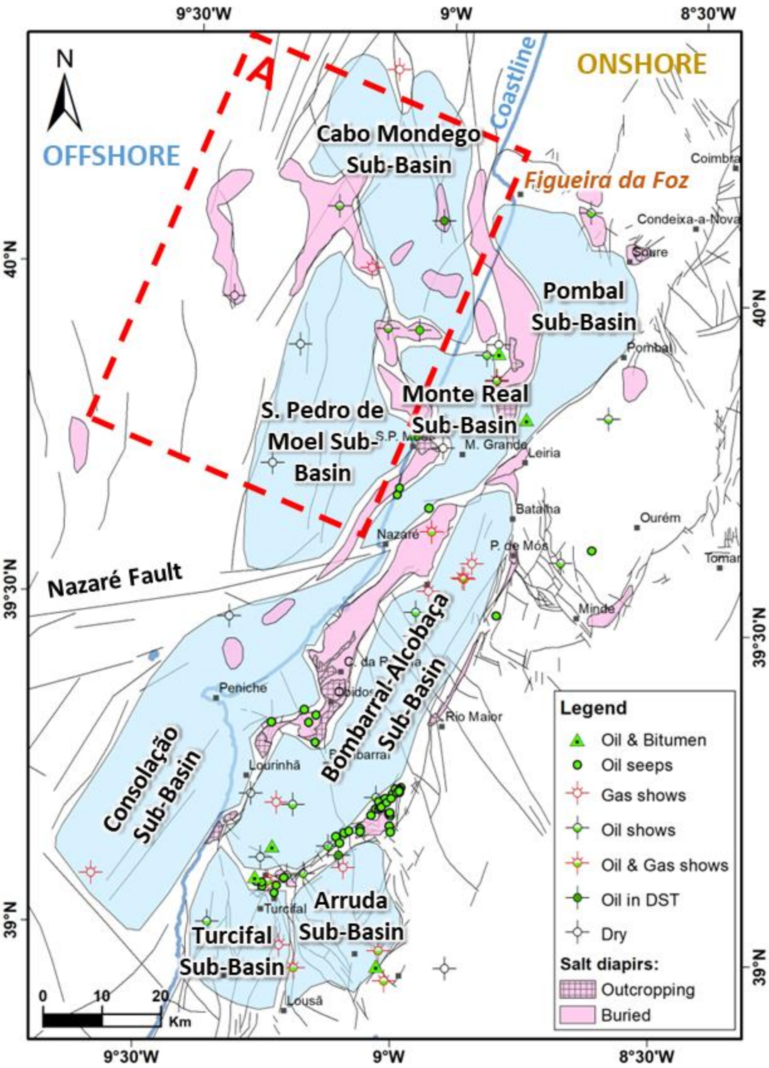

Figure 3: Location of the main sub-basins and salt diapirs in the Central/Northern sectors of the Lusitanian Basin (adapted from Casacão et al., 2023). The red dashed line delineates the location of the offshore study area.

The PilotSTRATEGY project has received funding from the European Union's Horizon 2020 research and innovation programme under grant agreement No. 101022664

The relationship between salt diapirism and deep basement faulting during the Jurassic extensional phases has been widely addressed in the LB (Zbyszewski, 1959; Wilson et al., 1989; Ribeiro et al., 1990; Pinheiro et al., 1996; Rasmussen et al., 1998; Alves et al., 2002). One of the examples of known salt diapirism is illustrated by salt pillow inflation on top of relative footwalls and relative basement highs controlled by Late Hercynian lineaments, associated with the salt withdrawal from the subsident hanging-walls, leading to the creation of broad sub-basins. The Late Jurassic rifting corresponded to the period of increased fault-controlled subsidence associated with salt movement, which developed the main sub-basins of *Arruda, Turcifal, Bombarral-Alcobaça and Consolação*, in the central sector, and the *Monte Real, Rio-Maior, Pombal and Cabo Mondego* and *São Pedro de Moel* sub-basins in the northern sector of the LB.

Subsequently to the Late Jurassic rifting event, leading to the creation of sub-basins and triggering salt diapirism, sedimentation carried out throughout the Lower Cretaceous, resulting in a thick package of fluvial-deltaic siliciclastic deposits, mostly sourced from the uplifted hinterland to the East. This important unit, considered as one of the most important reservoir targets in hydrocarbon exploration in the West Iberian margin (WIM), was named Torres Vedras Group. Seismic interpretation shows the extent of this seismic-stratigraphic unit, corroborated by well penetrations in the study area. However, its thickness and lithologies are likely to have been impacted by the existence of salt diapirs controlling the sedimentation routes. Two main types of salt diapir features were interpreted in the study area: salt pillows, not developing vertically into the formations overlying the Late Jurassic sediments, and inflated salt diapirs, bounded by elongated reverse faults reactivated during the Miocene inversion (drilled by the Espadarte (14A-1 and 14A-2) and Sardinha (13E-1 and 13C-1) wells).

As crustal stretching progressed throughout the Early Cretaceous, a basin-ward migration of the rift locus was recorded (Murillas et al., 1990; Alves et al., 2009), mostly due to continental crust thinning and rupture in the Upper Barremian, followed by exhumation and thinning of the upper mantle until the Aptian-Albian boundary (Soares et al., 2012). This later rift stage ultimately leads to the lithospheric breakup and the onset of seafloor spreading between the WIM and the Canadian Grand Banks since the Late Aptian (Pinheiro et al., 1996). The Albian to Cenomanian/Turonian lithospheric breakup final stage is developed on top of the Aptian breakup unconformity, which is particularly recognized in the LB.

Following the lithospheric breakup event, WIM entered the continental drift stage, with prograding siliciclastics deposited in the northern LB. Unlike in the southern LB, in the study area there is little evidence of the magmatic episode widely documented (e.g., Miranda et al. 2009; Pereira et al., 2020) that preceded the Cenozoic uplift phase. This tectonic inversion comprises two main events: 1) the Pyrenean phase, during the Eocene, and 2) the Betic phase, during the Miocene. This last compression phase played a critical role in salt diapirism in the LB, which resulted in the current configuration of the study area, through 1) rejuvenation of pre-existing salt pillows and domes over basement-related faults (Alves et al., 2003); 2) Hettangian salt acted as a décollement for thin-skinned tectonics (Ribeiro et al., 1990); and 3) rejuvenation and increased salt wall piercement, causing extrusion (Rasmussen et al., 1998).

The geometry and structural configuration of the study area can be summarized in a seismic cross-section (Figure 4), where the main storage complex elements are highlighted. The Dagorda salt unit (Hettangian) is seen to control the Jurassic, Cretaceous and Cenozoic *strata* thickness, as well as imposing a structural component that controls trap definition.

The PilotSTRATEGY project has received funding from the European Union's Horizon 2020 research and innovation programme under grant agreement No. 101022664

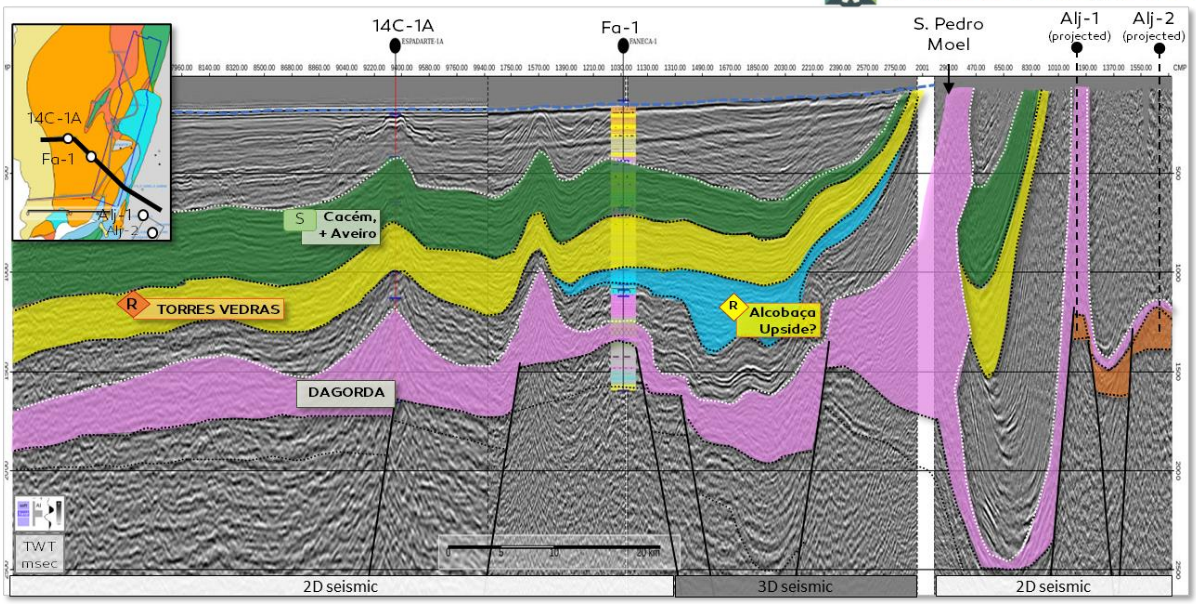

Figure 4: Structural configuration of the study area, resulting from the interpretation of a E-W seismic line. Main storage elements comprise the Torres Vedras Group (primary reservoir), the Cacém & Aveiro units (primary and secondary seals) and the Alcobaça Formation (secondary reservoir target). It is also interpreted the Dagorda salt unit (in pink), and the impact of diapirism in the creation of anticlines (structural traps).

3.2 Stratigraphy

The opening of the margin started with the onset of the Late Triassic rift event (Rift 1), with the sedimentation of intracontinental, fluviatile red beds, commonly known as the Silves Group (Palain, 1976; Witt, 1977; Wilson et al., 1989; Soares et al., 2012) in a set of half-grabens and grabens. The Silves Group is capped by an evaporitic/detritic sequence of Hettangian age, known as the Dagorda Formation (Palain, 1976), coheval (ca. 202-198 Ma) in west and southwest Iberia and northwest Africa (Davison et al., 2016). This unit is composed by alternating gypsum, halite, anhydrite, claystones and dolomite towards the top, deposited in a sabkha-type environment (Azerêdo et al., 2003), accessible in various outcrops in the LB and is the main source of salt diapirism (*sensu strictu*) in WIM. Its seismic facies are usually chaotic to transparent, resembling the seismic package of the underlying Triassic unit and Pre-Mesozoic acoustic basement, which poses interpretation constrains, particularly in deeper sections with poor seismic resolution. Nevertheless, the top salt unit is usually characterized by a strong seismic reflector corresponding to the overlying dolomitic member of the Coimbra Formation (Sinemurian), and its interpretation is also facilitated by deformed overburden strata onlapping against salt diapir geometries.

The Coimbra Formation marks the onset of the marine incursion in the LB (Azerêdo et al., 2003), that extends until the end of the Middle Jurassic. Coimbra Formation is constituted by dolomites and is overlain by the thick Brenha Formation (spanning between the Pliensbachian and the Callovian) that includes marlstones, limestones and marly limestones (Witt, 1977; Terrinha et al., 2019b). The transition to the Late Jurassic succession is made through a regional angular unconformity that resulted from tectono-eustatic controls also recognized in other circum-North Atlantic basins (Rasmussen et al., 1998; Azerêdo et al., 2002). The third major rift event resumed after this Callovian basin-wide event that endured until the Early Cretaceous, associated with mild crustal extension in

The PilotSTRATEGY project has received funding from the European Union's Horizon 2020 research and innovation programme under grant agreement No. 101022664

the LB. This rift episode corresponds to a period of continued extension, with reactivation of basement structures, erosion of rift shoulders, and deposition of transitional carbonates (Cabaços Formation), followed by open-marine limestones (Montejunto Formation) and fluvial, fluvio-deltaic (Abadia and Lourinhã formations) to turbidite accumulations (Leinfelder & Wilson, 1989; Pena dos Reis, 2000; Azerêdo et al., 2003).

The later rift stage during the Early Cretaceous ultimately leads to the lithospheric breakup and the onset of seafloor spreading between the WIM and the Canadian Grand Banks since the Late Aptian (Pinheiro et al., 1996; Dinis et al., 2008). During this time, interval deposition of shallow marine to fluvial sandstones occurred forming the Torres Vedras Group (TVG) depicted in Figure 5. The seismic facies of the TVG are transparent to high-amplitude continuous seismic packages attributed to coarse-grained to fine-grained siliciclastic sediments.

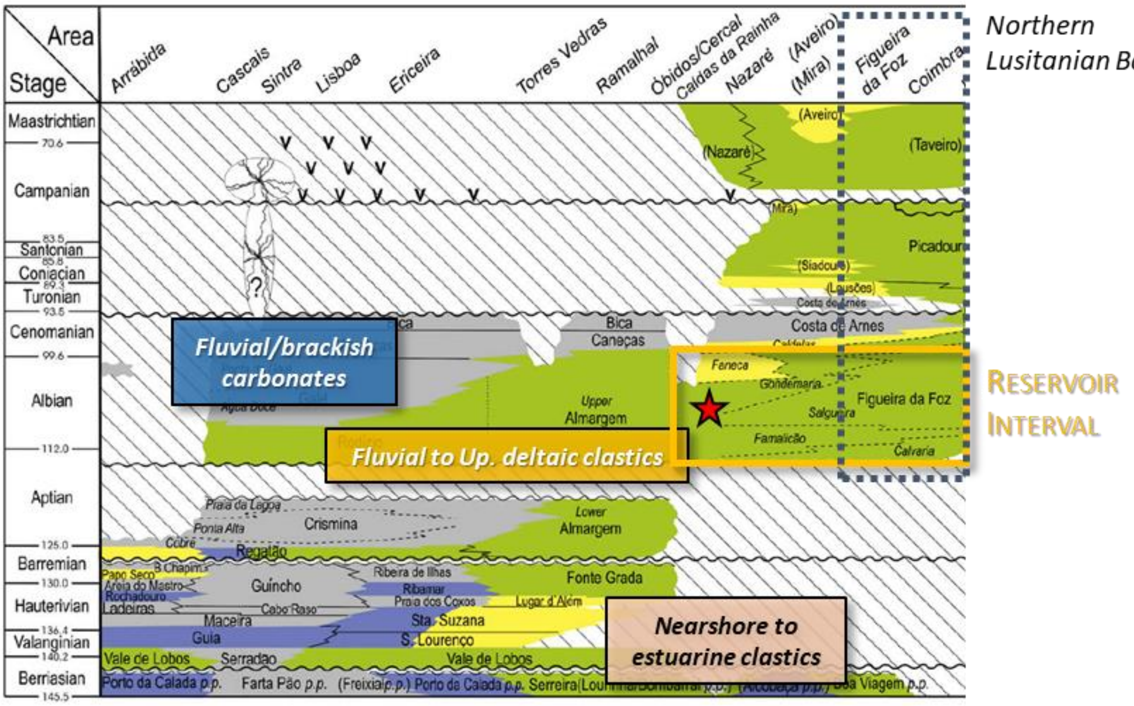

Figure 5– Synthetic lithostratigraphic chart of the Cretaceous of the Lusitanian Basin (modified after Dinis et al., 2008). Focus on the reservoir and seal intervals on the northern Lusitanian Basin (red star points out the stratigraphic position from which the outcrop pictures of Figure 34 were taken).

The Albian to Cenomanian/Turonian lithospheric breakup final sequence is particularly recognized in the LB, reflecting a fluvial depositional environment in its northern sector (Wilson et al., 1989; Rey et al., 2006; Dinis et al., 2008) overlain by shallow-marine carbonates associated with a Cenomanian-Turonian transgression (Witt, 1977), forming a unit commonly known as the Cacém Formation. By the Late Cenomanian, the LB was completely infilled, and the carbonate platform extended inland. Although the sedimentation during the Late Cretaceous was dominated by fluvial deposits, some marine layers are found in the early Turonian, Coniacian, Early Campanian and Maastrichian related to eustatic rises.

During the latest Cretaceous, a regional-scale alkaline magmatic event affected some Mesozoic basins of WIM with sub-volcanic intrusions and volcanic activity, although there is no evidence of this episode within the study area.

The PilotSTRATEGY project has received funding from the European Union’s Horizon 2020 research and innovation programme under grant agreement No. 101022664

Sedimentation continued throughout the Cenozoic, despite experiencing two main inversion events (e.g., Ribeiro et al., 1990). Cenozoic sedimentation occurred in a wide variety of environments like shallow marine, sub-littoral, deltaic or alluvial. Sandstones (coarse- to fine-grained) with layers of conglomerates or clays, siltstones, clays with layers of fine-grained sands, limestone are the most common lithologies found.

4. Storage Complex Characterization

As highlighted in the stratigraphic chart of Figure 2, the storage complex includes the main siliciclastic reservoir "Torres Vedras Group" (TVG) and the carbonate seal "Cacém Formation" (CF); sedimentation dated from the Early Cretaceous TGV to Late Cretaceous CF. A potential secondary seal composed mainly by fine-grained siliciclastics sediments (part of the Aveiro Group), of Upper Cretaceous age, overlies the storage complex. The Late Jurassic Alcobaça Formation, composed by fluvial to shallow marine siliciclastic sediments, has the potential to be a secondary reservoir, underneath the TVG and in hydraulic connection with it (no seal separates the two formations), but only as a theoretical candidate due to the lack of robust data and the absence of a seal other that the CF.

4.1 Log analysis and Petrophysics

For well log analysis and petrophysical evaluation, 12 vertical wells were considered, 7 offshore and 5 onshore, identified with a red circle in the map of Figure 6. The wells were drilled for petroleum exploration purposes and most of them spudded in the 1970s, with exception of Alc-1, that was drilled in 2012, MRW-5, MRW-8, and MRW-9, that were drilled in the 1960s, and Alj-2, that was drilled in the 1990s. As such, they have limited data acquisition and generally poor hole quality, which is illustrated through several washouts recorded in some of the most interesting formation targets. Table 1 summarizes the available logs used in the interpretation. For more detailed information on the petrophysical analysis conducted in the LB in the aim of this project, please refer to Deliverable 2.6.

The PilotSTRATEGY project has received funding from the European Union's Horizon 2020 research and innovation programme under grant agreement No. 101022664

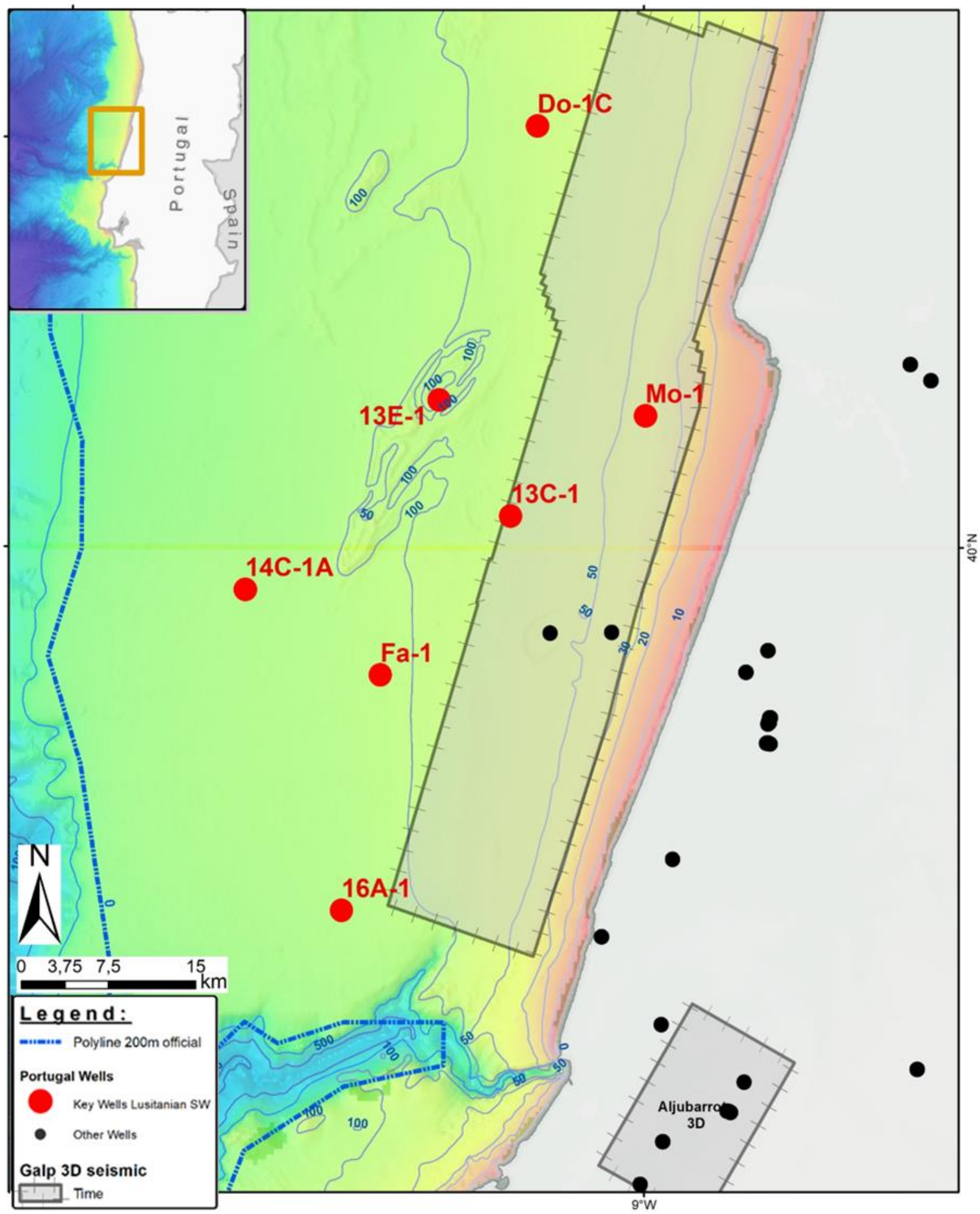

Figure 6: Basemap of the study area that includes the wells that were included for the petrophysical analysis (highlighted in red).

Several washouts were identified based on Caliper logs, which influences the log readings and increases the uncertainty in the petrophysical assessment. Due to the vintage character of some of the wells drilled in different exploration campaigns, and without routine core analysis and dynamic tests, it was impossible to calibrate the calculated porosities with 100% certainty. No image logs are present, which imposed additional difficulty in defining the sedimentary environment, paleocurrents, and data that could eventually be used to characterize tectonic stress (fractures/dips).

The PilotSTRATEGY project has received funding from the European Union's Horizon 2020 research and innovation programme under grant agreement No. 101022664

Table 1: Summary of the formations identified as potential reservoir intervals, and the available logs, per well.

	Well	Formation		Available Logs							
		Silves	Torres Vedras	Cal	GR	Spec GR	Den	Neu	Pef	Res	Dt
Offshore	Do-1C	x	x	x	x	-	x	x	-	x	x
	Mo-1	-	x	x	x	-	x	x	-	x	x
	13E-1	-	x	x	x	-	x	x	-	x	x
	13C-1	x	x	x	x	-	x	x	-	x	x
	14C-1A	-	x	x	x	-	x	x	-	x	x
	Fa-1	x	x	x	x	-	x	x	-	x	x
	16A-1	-	x	x	x	-	x	x	-	x	x
Onshore	Alc-1	x	-	x	x	x	x	x	x	x	x
	Alj-2	x	-	x	x	x	x	x	x	x	x
	MRW-5	-	-	-	x	-	-	x	-	x	-
	MRW-8	-	-	-	x	-	-	x	-	x	-
	MRW-9	-	-	-	x	-	-	-	-	x	-

Table 2 lists the pre-defined cut-offs used for net-to-gross (N/G) and net reservoir determination.

Table 2: Summary of the cut-offs applied in PHIE logs to identify seal and reservoir intervals.

Cut-offs	Curve	Value
Effective Porosity (Reservoir)	PHIE	> 8%
Effective Porosity (Seal)	PHIE	< 2%

Following the petrophysical analysis, some concluding remarks can be taken:

- Starting with the Late Triassic Silves Group, our analysis from the available wells suggests there is no minimum requirements to be considered as a potential reservoir, mainly due to extremely low N/G properties, combined with overall low porosity that does not exceed 10% (Table 3);
- Early Cretaceous TVG presents better N/G results, although with a large variability in the observed wells. This imposes an additional challenge for proper well correlation of sand packages within this unit. The TVG presents particularly good porosities, with an average value of 20% (Table 3). These combined properties and overall extension make this unit the best reservoir target to be pursued;
- Regarding the Late Jurassic Alcobaça Formation, petrophysical analysis was limited to the log suite available for the MRW-5 well, which did not allow full understanding of the reservoir characteristics. We, therefore, recommended to discard this unit as a target due to the lack of robust data quality and coverage to firmly consider it as an effective reservoir interval.

The PilotSTRATEGY project has received funding from the European Union's Horizon 2020 research and innovation programme under grant agreement No. 101022664

*Table 3: Summary with final petrophysical results, per well (*non-reliable result – only based on Neutron log).*

	Well Name	WD (m)	Top (MD m)	Bottom (MD m)	Gross (m)	Net (m)	N/G (%)	Av Phi (%)
TORRES VEDRAS FM.	Do-1C	84	880	1238	358	289	81	19
	Mo-1	45	703	1024	321	262	82	23
	13C-1	83	412	761	349	37	11	19
	13E-1	129	356	748	392	114	29	22
	14C-1A	133	802	1062	280	70	27	22
	Fa-1	112	860	1300	440	109	25	17
	16A-1	125	974	1472	498	320	64	17
SILVES Grp.	Do-1C	84	3525	3668	141	0.5	0.3	10
	13C-1	83	2459	2737	278	0.3	0.1	12
	Fa-1	112	2065	2597	532	1.4	0.3	9
	Alc-1	-	2653	3240	587	10.4	1.8	10
	Alj-2	-	3027	3616	589	-	-	-
Alcobaça	MRW-5	-	778	1084	306	305	99*	18*

4.2 Seismic Horizon and Fault interpretation in the Area of Interest

4.2.1 Dataset

The subsurface characterization of storage elements in the offshore Northern LB was conducted using 2D and 3D seismic datasets (Figure 7). Several 2D cross-sections in the LB were interpreted using different two-way time (TWT) vintage multi-channel migrated seismic surveys. A total length of 2950 km of 2D seismic reflection profiles, acquired by SSL/ESSO (1973), SSL/SHELL (1973), SEI/SUN (1974), GECO/NORAD (1980) and GSI (1984), were interpreted.

Subsurface analysis was complemented with the interpretation of the Cabo Mondego and São Pedro de Moel, a 3D seismic reflection volume acquired by Mohave Oil & Gas (2011) and located offshore Figueira da Foz (Figure 7).

In addition to seismic reflection data, information of ten wells (logs, formation tops, check shots) was used. Figure 7 illustrates the location of this set of legacy wells from petroleum exploration, operated by SUN, such as Mo-1 (1974) and Do-1C (1974), ESSO, such as Ca-1 (1974) and Fa-1 (1976), and SHELL for the remaining wells: 13C-1 (1974), 14C-1A (1975), 16A-1 (1975), 14A-1 (1975), 14A-2 (1976) and 13E-1 (1977). The set of available well log data is listed in Table 3.

The PilotSTRATEGY project has received funding from the European Union's Horizon 2020 research and innovation programme under grant agreement No. 101022664

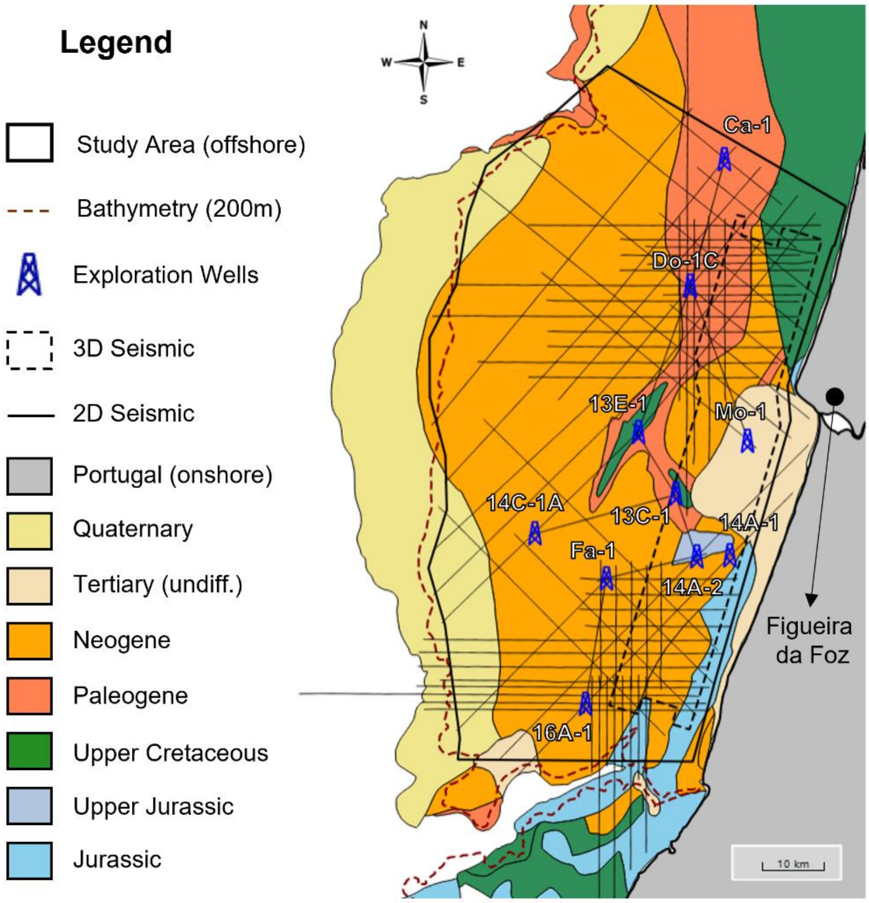

Figure 7: Dataset used in the characterization of the offshore study area, presenting the location of the wells, seismic reflection data (2D and 3D) and the offshore seabed geology (based on the Portuguese Geological Map 1:500 000, Oliveira et al., 1992).

4.2.2 Horizon and Fault picking

A total of six horizons were mapped in 2D and 3D seismic datasets, individualizing the main tectono-stratigraphic units of interest that characterize the storage elements (Table 4). The interpreted seismic horizons correspond to the Top Alcobaça Formation (~145 Ma), Top Torres Vedras Group (~100 Ma), Top Cacém Formation (93 Ma), Top Aveiro Group (~68 Ma), Top Espadarte Formation (50 Ma) and Seabed (0 Ma). Other seismic horizons between the Upper Jurassic and the Palaeozoic basement (Figure 8) were also interpreted for several seismic cross-sections, as Top Brenha Formation (~160 Ma), Top Coimbra and Upper Dagorda units (dolomites, ~195 Ma), Top Dagorda Formation (evaporites, ~199 Ma), Top Silves Group (~205 Ma) and Top Basement (~225 Ma). However, they are not presented herein as they are all stratigraphic units sitting below the main storage reservoir target, and therefore not relevant for the dimensioning of the storage complex. Nevertheless, the interpretation of the underlain formations was performed within the 3D seismic volume, and surface grids resulting from horizon picking will be integrated and handed over to the WP3 team to facilitate modelling.

The PilotSTRATEGY project has received funding from the European Union’s Horizon 2020 research and innovation programme under grant agreement No. 101022664

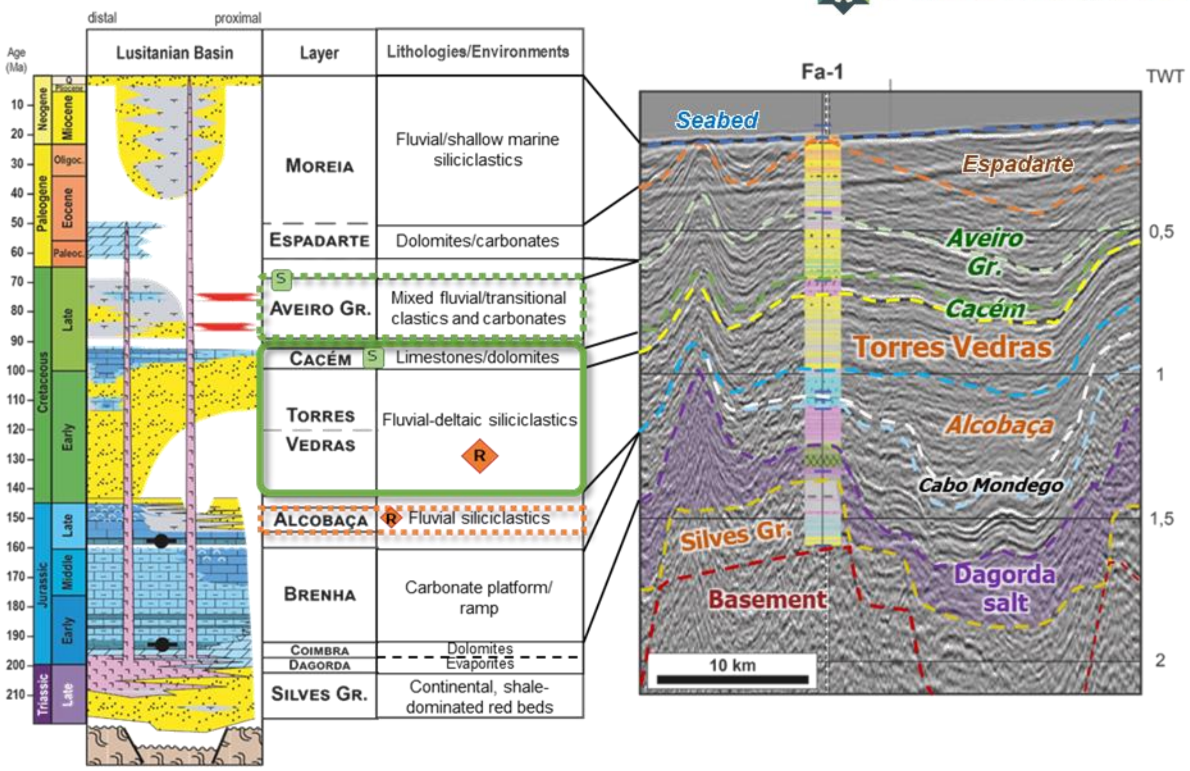

Figure 8: Lithostratigraphic chart of the Lusitanian Basin, its main tectono-stratigraphic units and a seismic screenshot with the main horizons that were mapped (Seabed, Top Espadarte, Top Aveiro Group, Top Cacém, Top Torres Vedras, and Top Alcobaça).

The first step consisted in a post-processing analysis of the 3D seismic volume (full-stack) to reduce the noise, increase the continuity of seismic reflectors, and improve the structures definition, which facilitated the seismic interpretation. The seismic-well tie process was conducted subsequently based on the synthetic seismograms of the wells located inside the 3D volume. Then, the horizons interpretation in the 3D post-processed volume was done using the seismic markers of formation tops of each well. The seismic display of 3D data is represented by a zero-phase wavelet and by the American (SEG) polarity convention with negative polarity representing a soft event. This is the case for the top of primary seal (Top CF), a regionally strong and continuous seismic reflector that was a key reference for seismic interpretation, while the reservoir top (Top TVG) is represented by a pick (hard event, positive amplitude). Other seismic horizons of the overburden zone, such as Top Espadarte Formation and Top Aveiro Group, were also interpreted as picks, while Top Seabed and Top Alcobaça Formation were interpreted as troughs. Due to issues with the original seismic processing, the seismic display in the shallower areas of the 3D volume is significantly poor and the interpretation of shallower seismic horizons (particularly Seabed), were performed recurring to several 2D seismic profiles available.

The interpretation of the 3D seismic volume identified several syncline and anticline structures at the top of the reservoir unit (TVG). Despite the broad extension of some identified synclinal structures, these were not considered preferential targets for a CO_2 storage site selection as fluid can easily migrate to shallower areas and compromise the retention capacity over time. In addition, several interpreted anticlinal structures within the 3D seismic volume were identified, despite being slightly shallower than the required threshold depths to secure long-term supercritical CO_2 fluid phase. Nonetheless, a few anticlinal structures were interpreted west of the 3D seismic volume and identified

The PilotSTRATEGY project has received funding from the European Union's Horizon 2020 research and innovation programme under grant agreement No. 101022664

as promising for CO_2 storage. To confirm its presence and extent of these anticlines, an additional set of 2D seismic profiles was interpreted.

Before extending the interpretation of the tectono-stratigraphic elements of the storage complex to this western offshore area of the basin, 3D-2D seismic-well tie process was conducted. This task followed a sequential procedure, correcting and uniformizing the time, phase, and amplitude discrepancies between datasets. The seismic tie process was firstly performed between the 3D volume (reference volume) and all the 2D seismic profiles that intersect it. Then, each set of 2D profiles from each seismic campaign were tied simultaneously to the previous 2D profiles whenever mis-ties of each set were similar (when not, the tie process was made one-by-one). The same sequential procedure was performed for the remaining 2D profiles until mis-ties between all seismic datasets was satisfactory (i.e., up to 50 ms between 2D seismic profiles that display poor data quality).

Fault interpretation was conducted, and fault intersection outlines were made for different seismic horizons. The interpretation of existing faults in the offshore area of interest was firstly done in the 3D seismic volume. Several seismic attributes were also computed, e.g., coherency, to better identify and interpret the discontinuities present within the 3D seismic volume. After integrating the additional set of 2D seismic profiles, as mentioned previously, the continuity of several faults adjacent to the limits of the 3D volume was possible to be tracked. It is important to mention that the interpreted faults in the westernmost zones of the study area present higher uncertainty, due to the lack of seismic data (based on few 2D seismic profiles only), when compared to those mapped in the eastern part using both 2D and 3D seismic data. Regarding primary seal and reservoir, a total of 24 faults were identified and interpreted for the whole offshore area under study (Figure 12 and Figure 13). In general, the faults strike N-S and NW-SE, with exception of a couple of faults inside the 3D volume that are oriented W-E. Most of the interpreted faults are normal faults, while the presence of reverse faults is typically associated to the halokinesis in the basin, leading to the generation of uplifts (structural highs) in several zones. The throws of these faults are significantly high (i.e., several hundreds of meters). Throws of normal faults associated with the boundaries of the main graben structure in the northeast of the study area (close to the selected storage site) are also high (in the order of several hundreds of meters), although the other fault throws of the half-grabens are relatively small (dozen to a few hundreds of meters). For the remaining normal faults identified, the throws are in general relatively small (dozen to a few hundreds of meters), excepting a sub-vertical normal fault in the structural high of well 13C-1 (Figure 13), whose fault throw is significantly high with depth (from dozens of meters in the shallower Cretaceous units to several hundreds of meters towards the basement), being associated with the development of one of the sub-basins present in this study area.

After completing the interpretation of the tectono-stratigraphic elements, the set of seismic horizons were mapped to obtain the structural maps (in TWT) as well as the fault picks to generate the fault polygons (t-surfaces). These elements were used as inputs elements in the generated velocity model for the time-depth conversion procedure.

4.2.3 Time-Depth conversion

The velocity model used for time-depth conversion was generated based on the interval velocities between the stratigraphic tops from available wells. Different velocity models were tested according to the interval velocities of several wells, as well as the average values between them for each stratigraphic unit. The available migration velocity model for the 3D seismic volume, was also initially

The PilotSTRATEGY project has received funding from the European Union’s Horizon 2020 research and innovation programme under grant agreement No. 101022664

considered for time to depth conversion. However, this 3D velocity model was discarded as the resultant depth maps showed several geological inconsistencies, both in the shallower and deeper areas.

The final interval velocities used for the time-depth conversion are listed in the Table 4. A global velocity model, following the structure of the seismic horizons ("layer cake model"), was used for the conversion process of the seismic horizons and fault polygons. The converted surfaces were cross-checked with the tops of stratigraphic units at the well location, resulting in a reasonably good match, particularly for the primary seal and reservoir tops in which the mismatch was about 20 m. These discrepancies between the seismic results and the well data are due to the uncertainties in the velocity model itself but also due to the uncertainties carried out from the horizons picking away from the wells and the surfaces mapping that always smooth the seismic horizons.

Table 4: Summary of the interval velocities (m/s) considered for each interpreted unit.

Seismic Horizons	Interval Velocity (m/s)
Seabed	1650
Espadarte Formation	2200
Aveiro Group	2650
Cacém Formation	4300
Torres Vedras Group	3350
Alcobaça Formation	3600

4.2.4 Depth top structure maps

The final structural maps in depth (meters), considering the no deposition/erosion areas and the intersections of the faults for each surface, are illustrated from Figure 9 to Figure 14. These maps allowed the subsequent dimensioning and characterization of the target anticlinal structures.

The PilotSTRATEGY project has received funding from the European Union's Horizon 2020 research and innovation programme under grant agreement No. 101022664

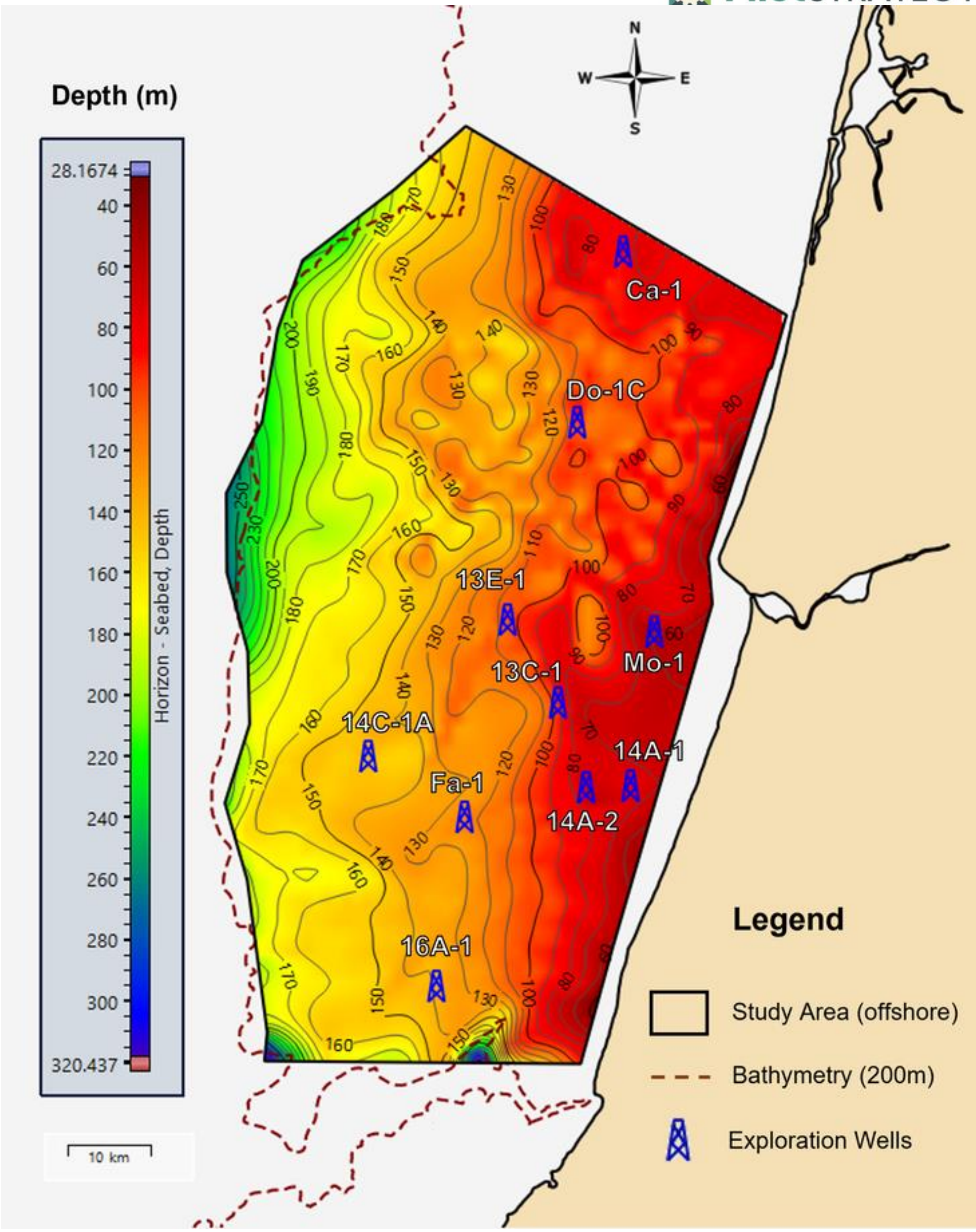

Figure 9: Structural map (in Depth) of the Seabed in the offshore study area. Isolines of 10 meters.

The PilotSTRATEGY project has received funding from the European Union's Horizon 2020 research and innovation programme under grant agreement No. 101022664

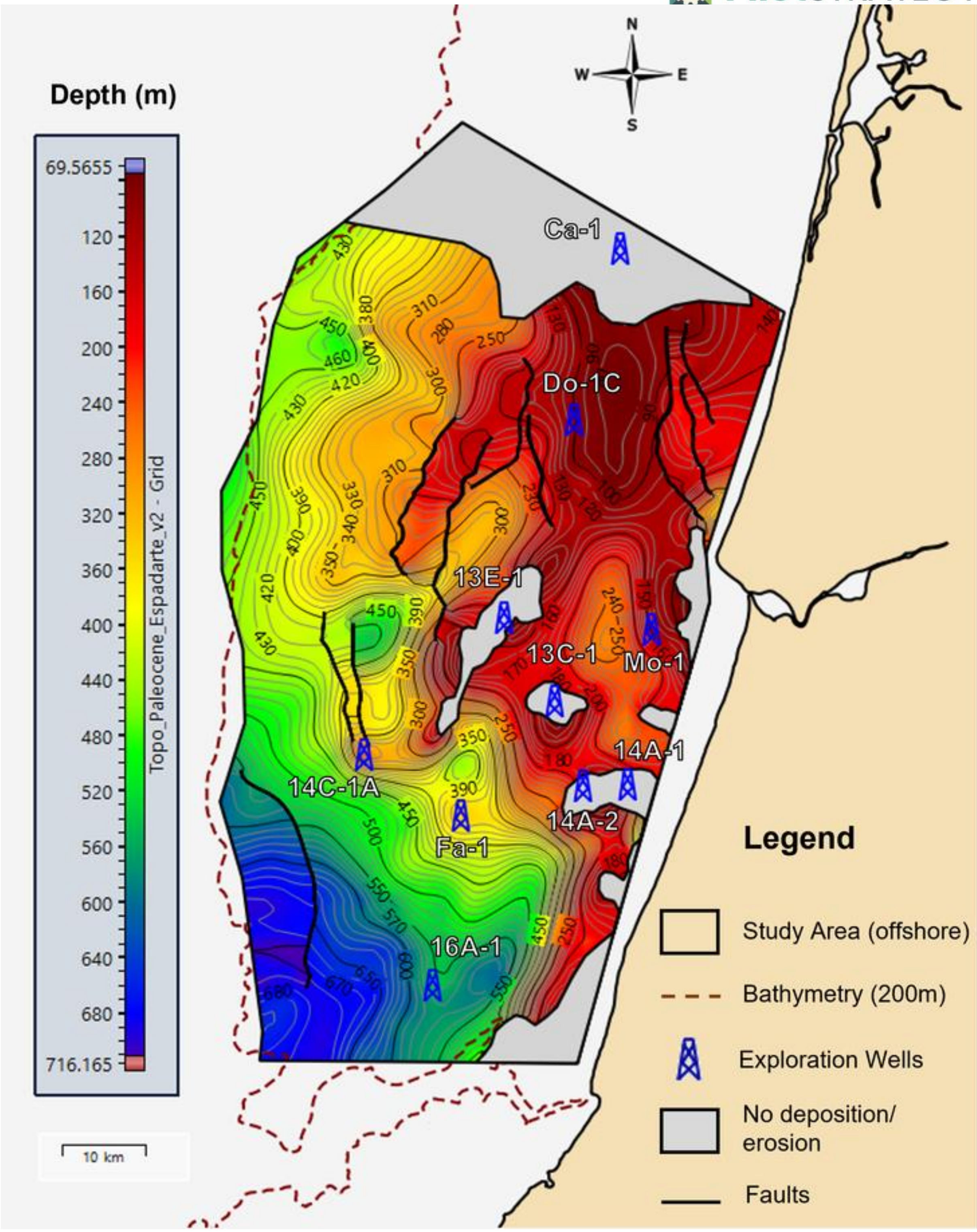

Figure 10: Structural map (in Depth) of the Top Espadarte Formation in the offshore study area. Isolines of 10 meters.

The PilotSTRATEGY project has received funding from the European Union's Horizon 2020 research and innovation programme under grant agreement No. 101022664

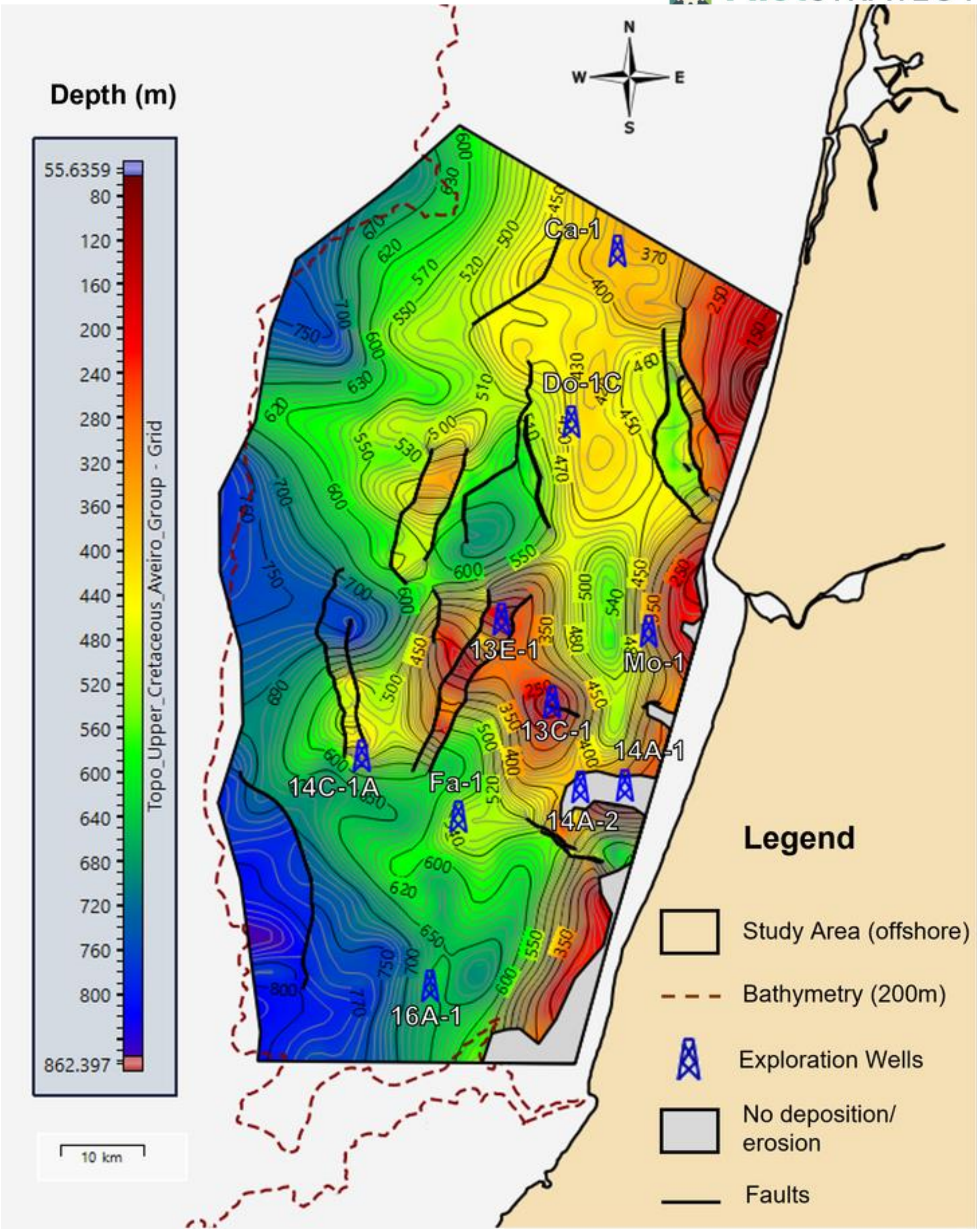

Figure 11: Structural map (in Depth) of the Top Aveiro Group in the offshore study area. Isolines of 10 meters.

The PilotSTRATEGY project has received funding from the European Union's Horizon 2020 research and innovation programme under grant agreement No. 101022664

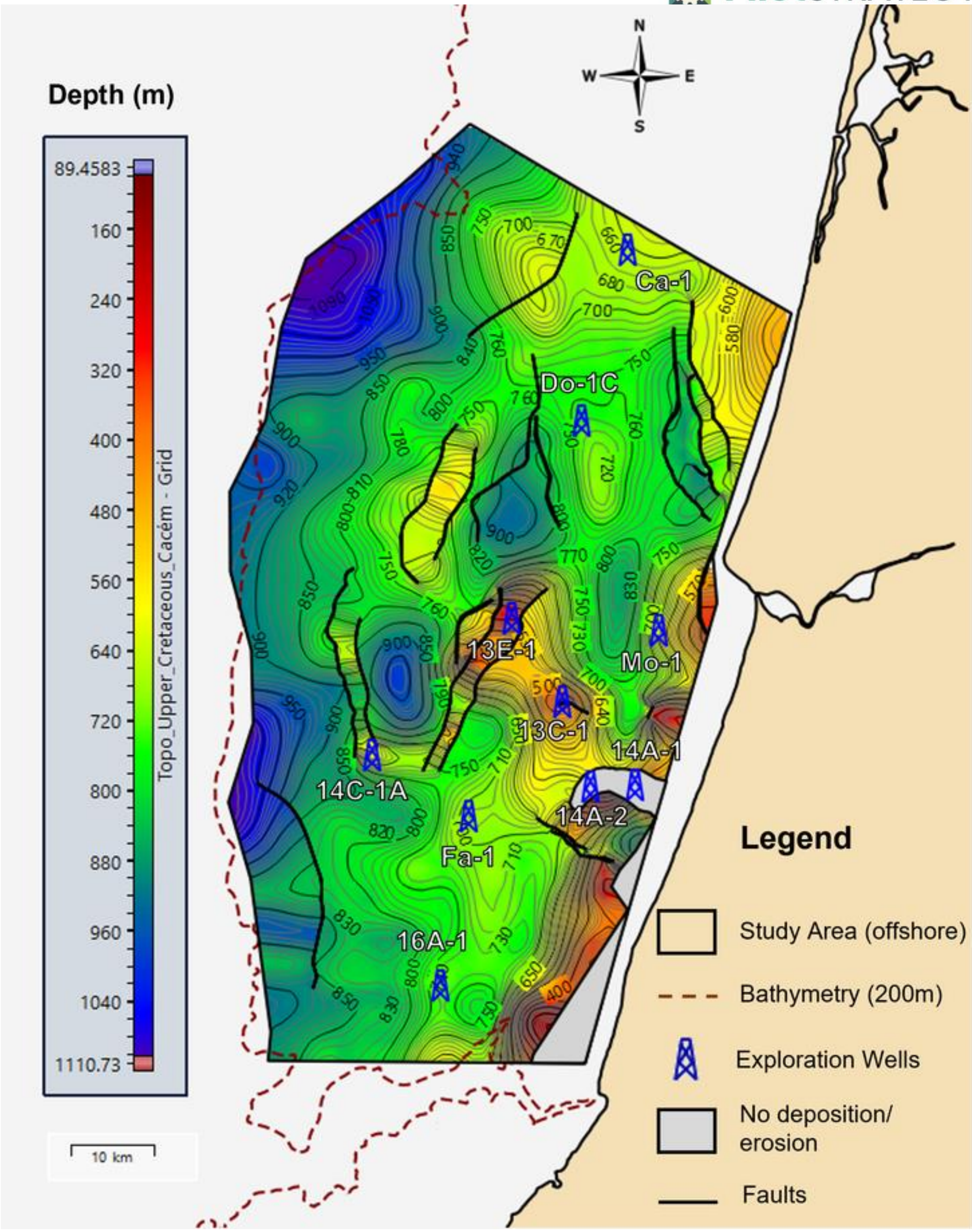

Figure 12: Structural map (in Depth) of the primary seal (Top Cacém Formation) in the offshore study area. Isolines of 10 meters.

The PilotSTRATEGY project has received funding from the European Union's Horizon 2020 research and innovation programme under grant agreement No. 101022664

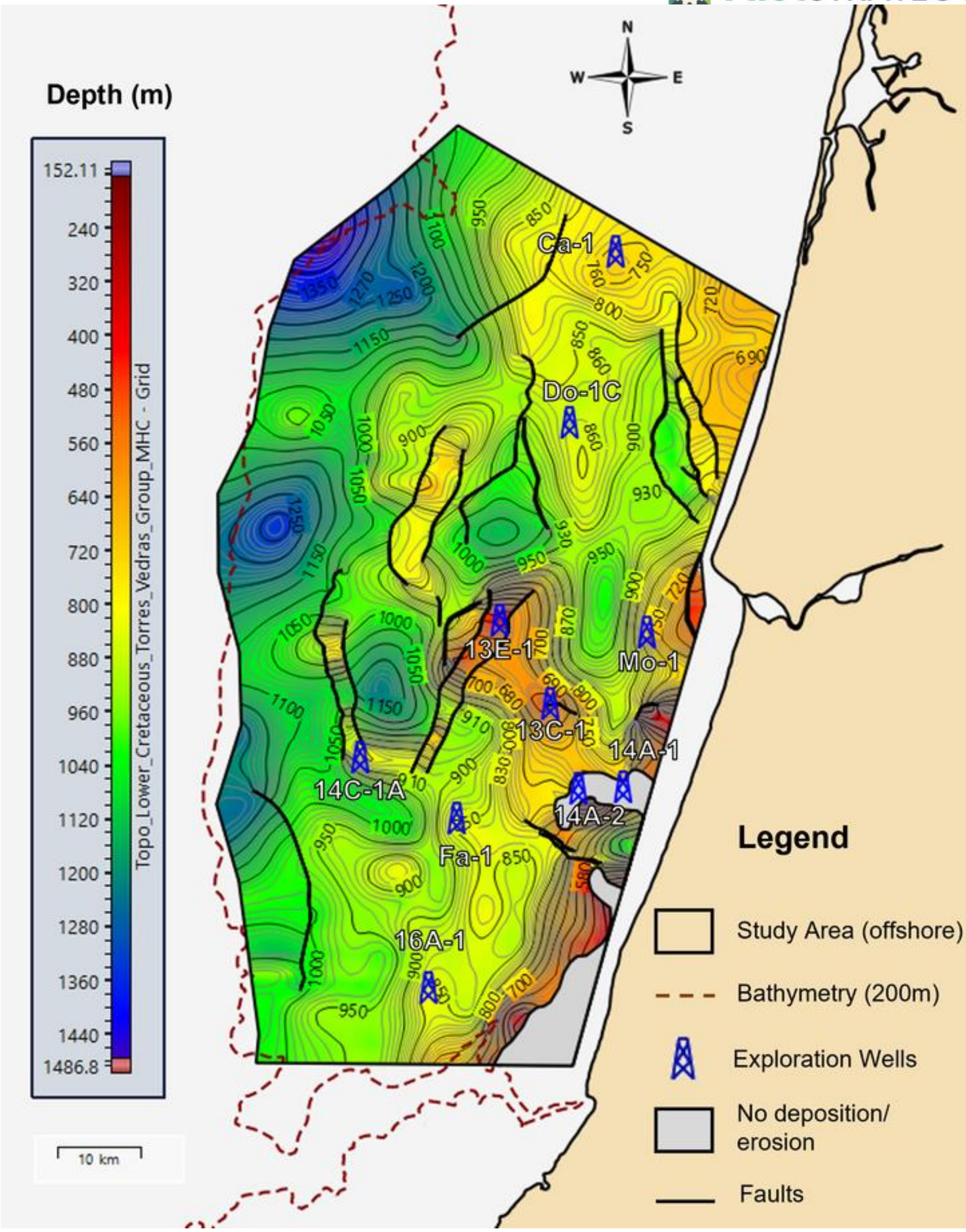

Figure 13: Structural map (in Depth) of the top of reservoir (Top Torres Vedras Group) in the offshore study area. Isolines of 10 meters.

The PilotSTRATEGY project has received funding from the European Union's Horizon 2020 research and innovation programme under grant agreement No. 101022664

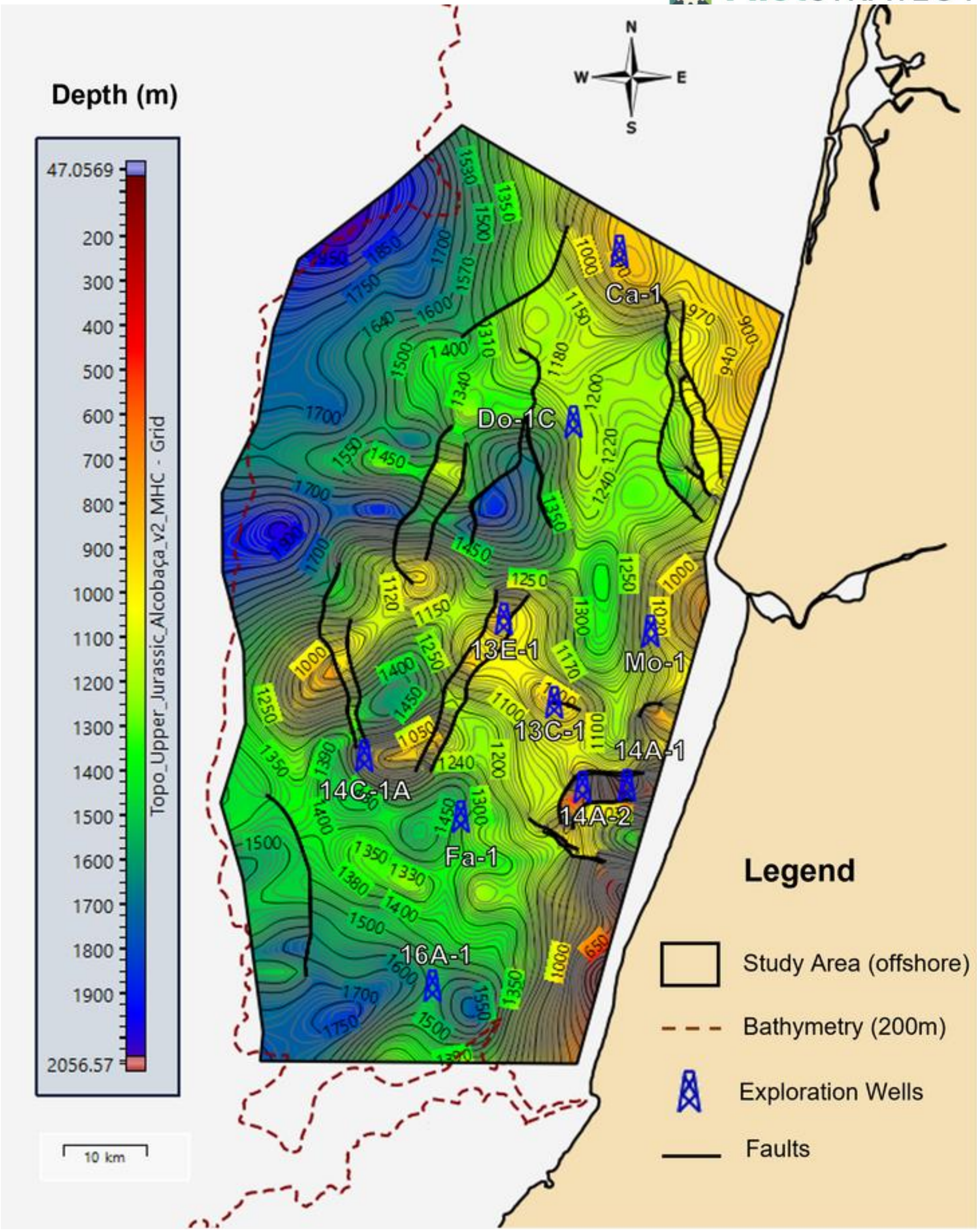

Figure 14: Structural map (in Depth) of the base of reservoir (Top Alcobaça Formation) in the offshore study area. Isolines of 10 meters.

4.3 Additional Geophysical Surveys

4.3.1 Regional Magnetic Interpretation

For the evaluation of the LB (offshore and onshore coastal areas), airborne magnetic data surveyed by Mohave Oil & Gas, in June-July 2011, were interpolated using minimal curvature method with cell size of 250 meters and corrected by adequate IGRF (International Geomagnetic Reference Field) model of year 2010 (UTS Aeroquest Airborne, 2011) (

Figure 15). Due to inclination and declination of the magnetic field, it was necessary to carry out a process called Reduction to Pole (Baranov, 1964), which numerically transpose the data to Earth's magnetic pole and verticalize the magnetic anomalies.

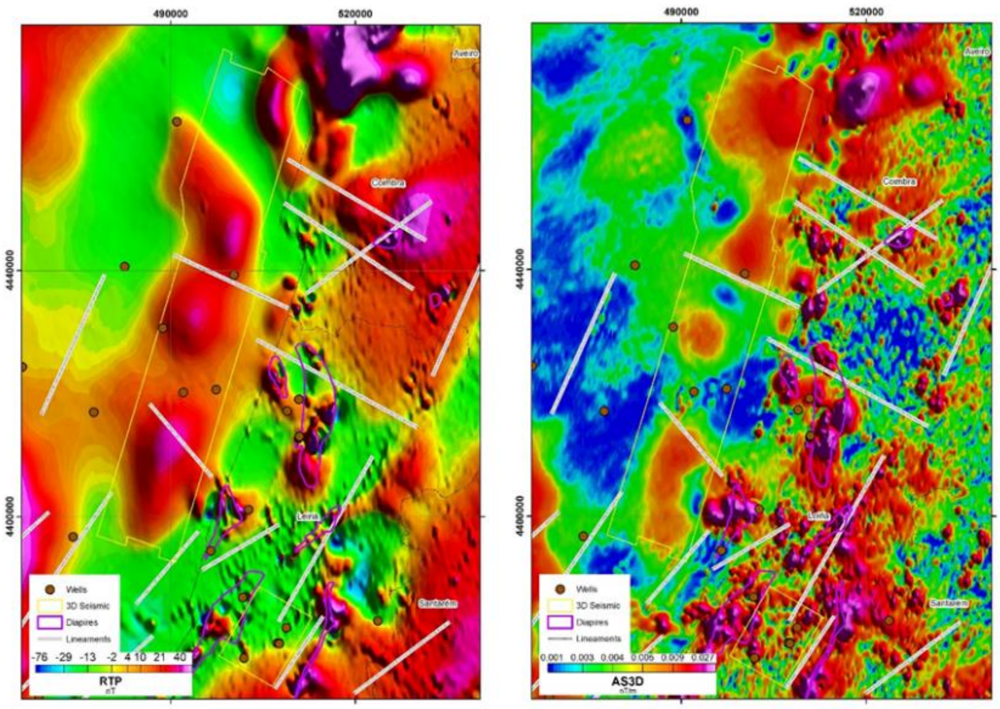

Figure 15: Detailed maps of magnetic data reduced to pole (left) and analytic 3D signal (right), containing lineament extractions on Lusitanian Basin, 3D seismic blocks and diapirs in the region of most interest.

Associated to Reduction to Pole (RTP), the 3D Analytic Signal (Li, 2006) were performed. The concept of this technique was introduced by Roest et al. (1992) as a three-dimensional vector which contains the horizontal and vertical derivatives and their Hilbert transform, providing the analytic signal amplitude in a horizontal plane. Therefore, magnetic contents in geological features could be mapped as lineaments and associated to structures (Isles & Rankin, 2013).

The results of lineaments extractions are presented in

Figure 15, in RTP and Analytic Signal maps. As observed, it is possible to identify the main lineaments from the maps of magnetic data reduced to pole and analytic 3D signal in the study area. These lineaments are mainly related to deep basement's structures but also retain information of sedimentary contents due to different signatures in the magnetic maps and profiles (Gunn et al., 1997; Oliveira et al., 2018).

The PilotSTRATEGY project has received funding from the European Union's Horizon 2020 research and innovation programme under grant agreement No. 101022664

4.3.2 Passive Seismic

Passive seismic method is commonly known as the record and analysis of natural or induced seismicity with borehole or surface sensors (seismic monitoring) but also includes the acquisition of ambient vibrations, without using any active energy sources. Seismic monitoring is traditionally used in CO_2 storage projects to image the injected CO_2 plume and detect seismicity related with the CO_2 injection (Maxwell and Fabriol, 2004; Lumley et al., 2014; Sutherlan et al., 2022)

In this project, as a way to control costs and simplify the acquisition process, an experimental campaign of passive seismic using ambient noise was additionally used as a source of data to subsurface characterization. Passive seismic techniques based on ambient noise vibration are a cost-reduced methodology, when compared with the acquisition of common active seismic and cheaper than drilling a well. Furthermore, it has lower environmental impact than active seismic which require a strong source of seismic wave (e.g., dynamite or vibroseis). These advantages are valuable, not only for the early characterization of the site storage capacity, but also for the future monitoring of CO_2 injected plume.

The autocorrelation method consists of extracting the subsurface reflectivity from the autocorrelation of ambient noise time windows and subsequent stacking (Benjumena et al., 2022; Zhao et al., 2022). Seismic data was recorded during a few days to form time series long enough to observe the seismic behaviour underneath the seismic stations. Using the vertical component, the time series was then stacked into one single trace for each station, comparing signals of a station to itself in different phases and slight time shifts. The single trace of every station was subsequently compiled in a profile that allows to detect reflectors in subsurface.

Two passive seismic campaigns were conducted onshore: the first in São Pedro de Moel area and a second one in Monte Real area (Figure 16). These areas are located onshore but in the proximity of the offshore selected site, as such bringing value to the understanding of the pilot injection site. The two campaigns had different objectives: the first one aimed to test the possibility to connect both offshore and onshore 3D volumes, whereas the objective of the second campaign was to improve the characterization of the TVG unit in the onshore, considered as an analogue for the offshore target area.

The first campaign carried out in the São Pedro de Moel area (Figure 17) aimed to investigate the applicability of this method to the LB taking advantage of the existing drilling and seismic reflection profile. Seismic noise data was collected by five Broadband Seismic stations, one located near the SPM-2 well and the others disposed along a seismic profile. The recordings were made over three days using Guralp CMG 6TD stations. The results show that, both along the survey and along the profile, there is a good relationship between the pre-existing data and the data obtained from the ambient noise profile.

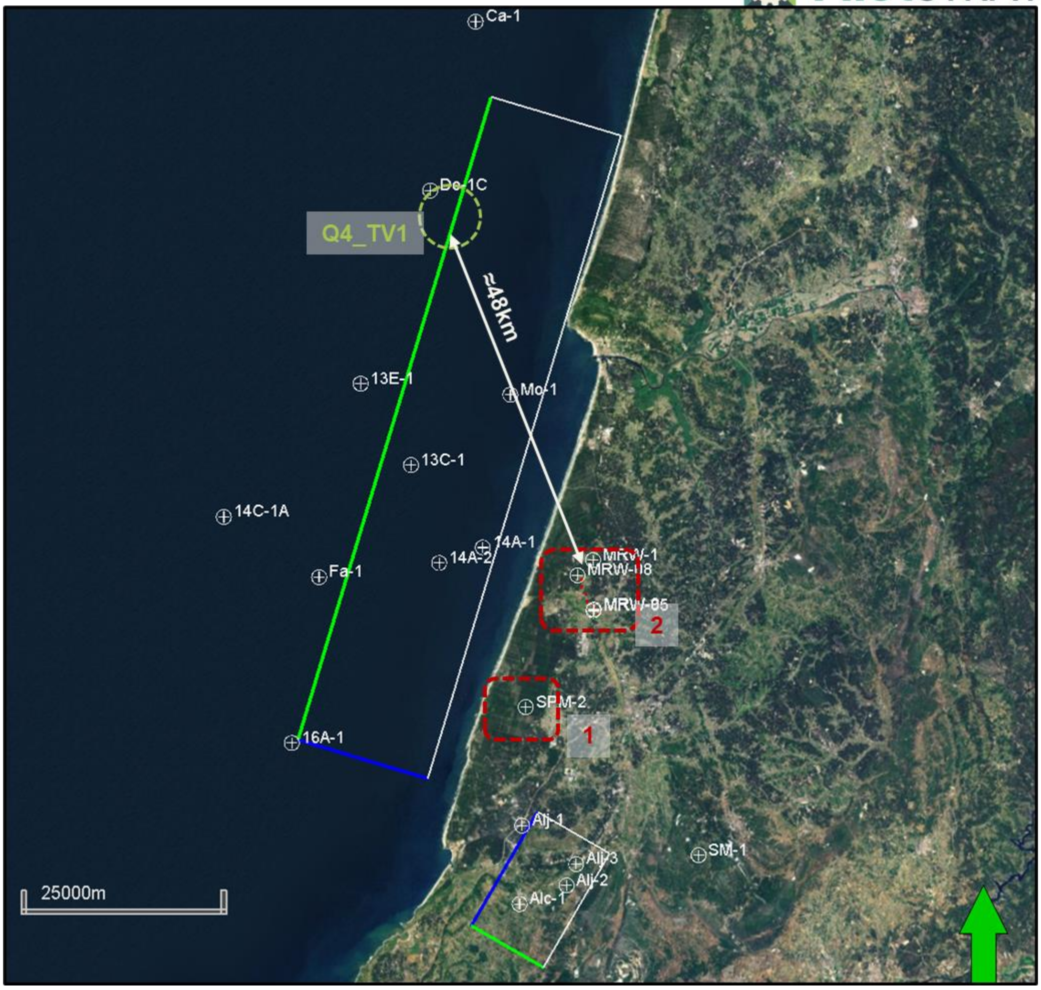

Figure 16: Location of the onshore passive seismic pilot campaigns: 1) São Pedro de Moel campaign; 2) Monte Real campaign. Q4-TV1 corresponds to the selected prospect location (please refer to Figure 24 and section 4.5 for more details).

Figure 17: Geographic location of SPM-2 well and 2D seismic profile used as reference in São Pedro de Moel passive seismic campaign.

The PilotSTRATEGY project has received funding from the European Union's Horizon 2020 research and innovation programme under grant agreement No. 101022664

The second campaign of passive seismic ambient noise survey in the Monte Real area was conducted with the goal to assess the potential cross-interpretation of the autocorrelation results with seismic reflection data and wells. Additionally, the team wanted to test its potential for possible larger scale applications. This data may be relevant especially in an early-stage site assessment where there is limited well and seismic datasets to evaluate the continuity, depth and thickness of the geological features observed in scarce 2D seismic lines.

The Monte Real site is located onshore of LB, in central Portugal, approximately 8.5 km from the coast. Monte Real is a good analogue for the offshore area, where the storage complex is being assessed, considering the TVG reservoir characterized onshore. The top of the thin carbonate/marl-rich layer (seal CF) was here also interpreted as a strong seismic reflector. The Monte Real area is characterized by the existence of a prominent salt-wall bounded by a few faults, formed by diapirism throughout the Mesozoic and Cenozoic, crossed by some of the deployed seismic stations.

The passive seismic data acquisition was designed to assess the storage potential, and, for quality control, stations were deployed in the vicinity of boreholes and legacy seismic reflection lines. Fifteen seismic stations were positioned with an approximate spacing of 350 m, along a line that connects 2 wells in the area and that ties to three legacy 2D seismic reflection lines (Figure 18). However, only 13 out of the 15 stations have reliable data, as stations 3 and 6 have recorded useless noise data imposed by human activities. The acquisition lasted for 5 days, and the seismic sensors were buried at approximately 50 cm deep in the ground (a few places with unconsolidated sands).

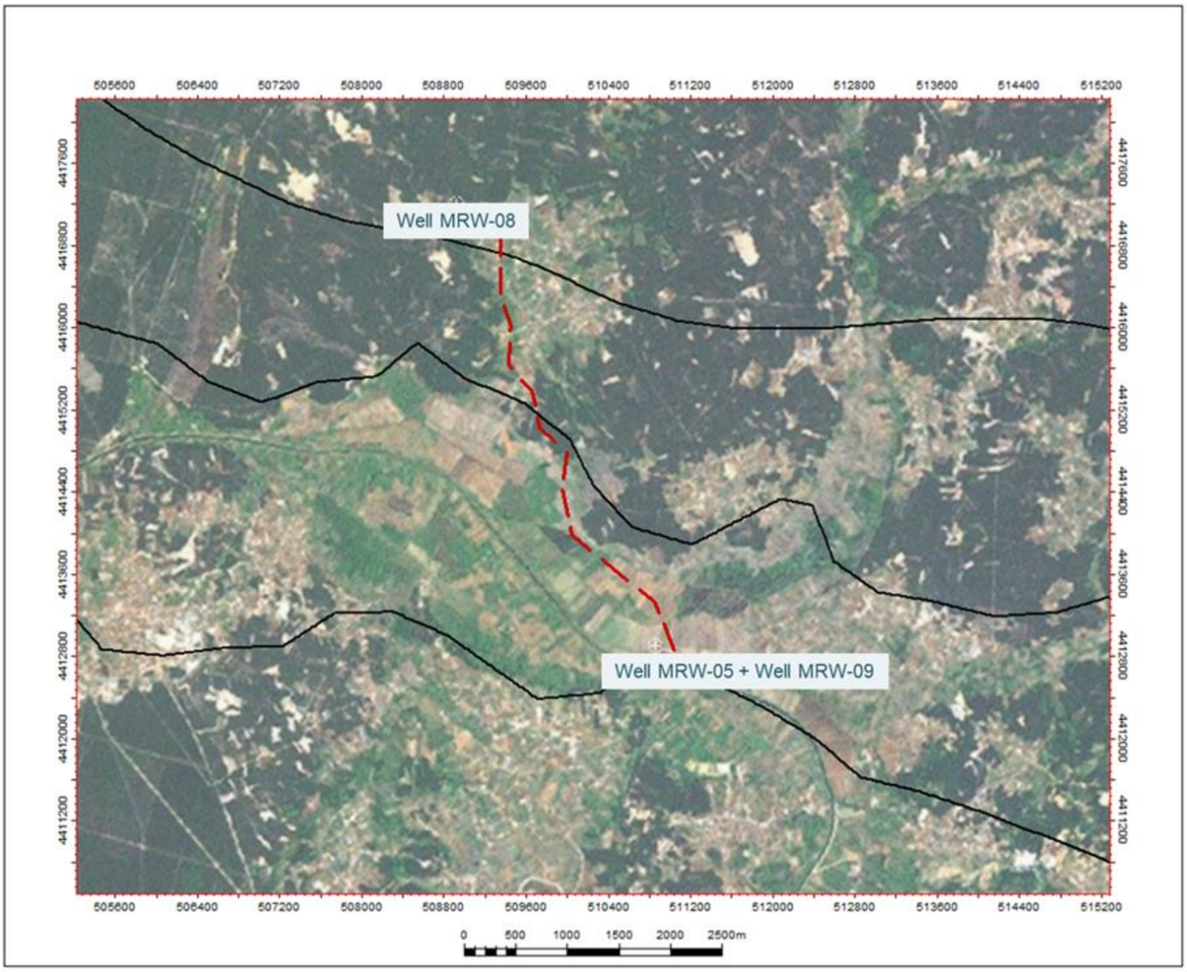

The PilotSTRATEGY project has received funding from the European Union's Horizon 2020 research and innovation programme under grant agreement No. 101022664

Figure 18: Satellite image overlaid with the array of seismic stations (dashed red) and legacy 2D seismic lines used in this study (black).

The several traces resulting from the autocorrelation were compiled in one pseudo 2D line that was integrated in the local interpretation. It was observed that the traces from stations located close to the wells capture the strong seismic events that match the main reflections observed in the 2D lines. Although the recorded signal captures the ambient noise coming from the subsurface, several surface noise sources in this area that may have interfered with the recorded data are observed. Some of the stations were placed closed to strong noise sources such as trees, electric lines, water pumps and farm equipment. Moreover, there is an airport located nearby the area of study. Even though this area is located away from big urban areas, the acquisition line crosses agricultural zones and intersects a village.

The pseudo 2D line obtained from autocorrelation intersects three legacy 2D seismic lines (all in E-W direction) and provides additional information along the N-S direction, crossing the possible anticlinal observed in the legacy maps and the Monte Real salt diapir. It was included in the horizon picking workflow by creating composite seismic lines with the legacy 2D seismic reflection lines, adding important information to improve the quality of the picking where legacy seismic is lacking (Figure 19). Efforts were done to keep conformity among the picking of different horizons, but the interpretation was affected by low data quality and faulted geological setting. Some reflectors look more chaotic probably cause by the effect of the salt, and the picking holds a good level of irregularity and uncertainty. Nevertheless, the analysis of the preliminary results of this autocorrelation pilot indicates that the methodology has a strong potential to be applied to the characterization of geological sites for CO_2 storage, especially in areas with limited data available.

Even though the interpretation constraints caused by the weak body wave of the ambient noise, which makes it difficult to distinguish between signal and multiples in the imaging results, the main impedance reflectors were observed in the traces and compared with the seismic reflection data. Moreover, the image obtained was integrated with the interpretation workflow and the horizon picking has improved, due to the additional information in terms of continuity.

The PilotSTRATEGY project has received funding from the European Union's Horizon 2020 research and innovation programme under grant agreement No. 101022664

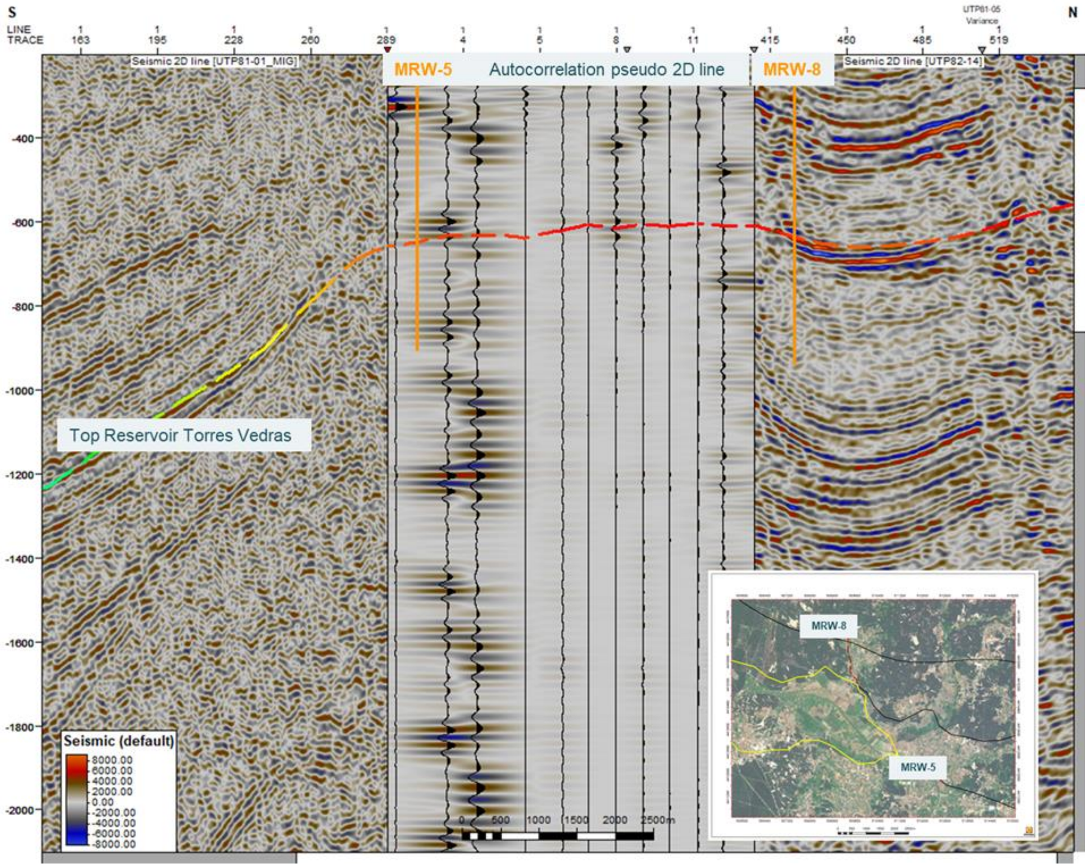

Figure 19 – Seismic section showing a composite line that includes the autocorrelation 2D line. The top of the reservoir is plotted, and it's observed its continuity along the lines

4.4 Well-Seismic Stratigraphic Correlation

As previously mentioned in section 3.2, the play that defines the CO_2 storage complex is composed by the TVG reservoir (Aptian?-Albian), which is capped by a seal unit of the CF (Cenomanian-Turonian), and a potential secondary seal, part of the Aveiro Group (Late Cretaceous). Underlying the TVG sandstones, a secondary reservoir of the Late Jurassic (Alcobaça Formation) can also be considered with no seal identified between the two formations.

Figure 20 shows an NNE-SSW seismic section crossing the Ca-1, Do-1C and 13E-1 wells, highlighting the main structural features. As observed, the main reservoir from TVG is laterally continuous and is thinning (pinch-out) towards the Ca-1 well (NNE direction), which represents a stratigraphic trap. This is in accordance with what was observed in section 4.5 easing to define the P10 outline of the Q4-TV1 structure, highlighted as the main prospect to focus in WP3. This package is mainly composed by siliciclastic sediments, primarily sandstones (Pereira et al., 2022), and encompasses intra-reservoir claystones, as observed in the gamma-ray (GR) logs. The CF seal is composed by limestones, marls and clays, and is continuous and homogenous over the area of interest, showing strong amplitudes in the seismic section and low inferred porosity (low GR), as is seen in Figure 20. This GR-trend is observed in all well correlations (Figure 21), in which the lower part of CF shows a higher GR content and its upper section shows slightly lower GR values and lower porosity, which is supported in literature and well reports by the limestone/dolomite-rich facies of this sealing unit (Figure 22).

The PilotSTRATEGY project has received funding from the European Union's Horizon 2020 research and innovation programme under grant agreement No. 101022664

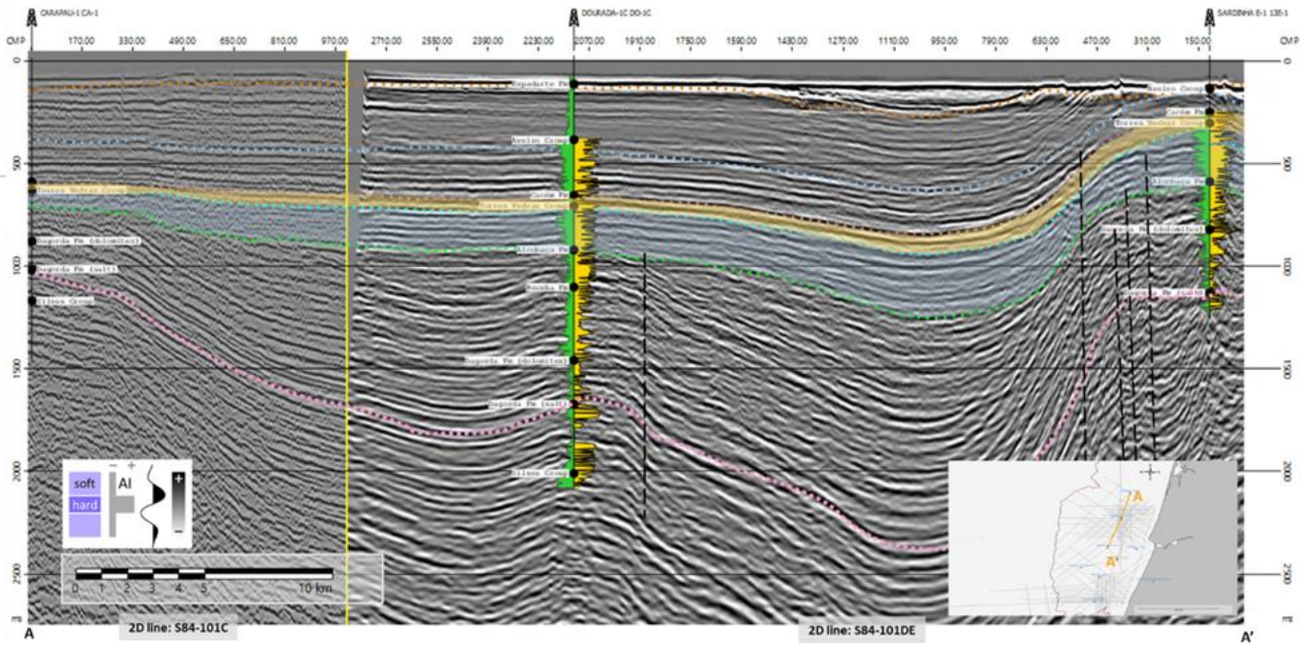

Figure 20: NNE-SSW seismic section crossing the wells Ca-1 (left), Do-1C (middle) and 13E-1 (right) and showing the Gamma-ray (GR) logs in green and the effective porosity logs (PHIE) in yellow.

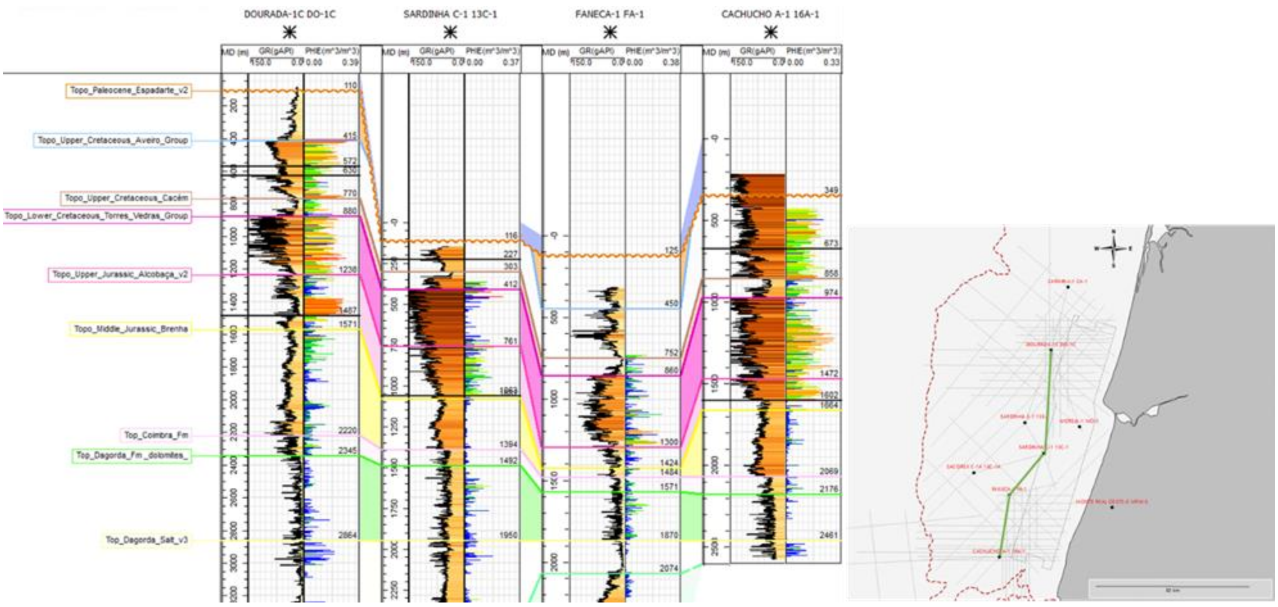

(a)

The PilotSTRATEGY project has received funding from the European Union's Horizon 2020 research and innovation programme under grant agreement No. 101022664

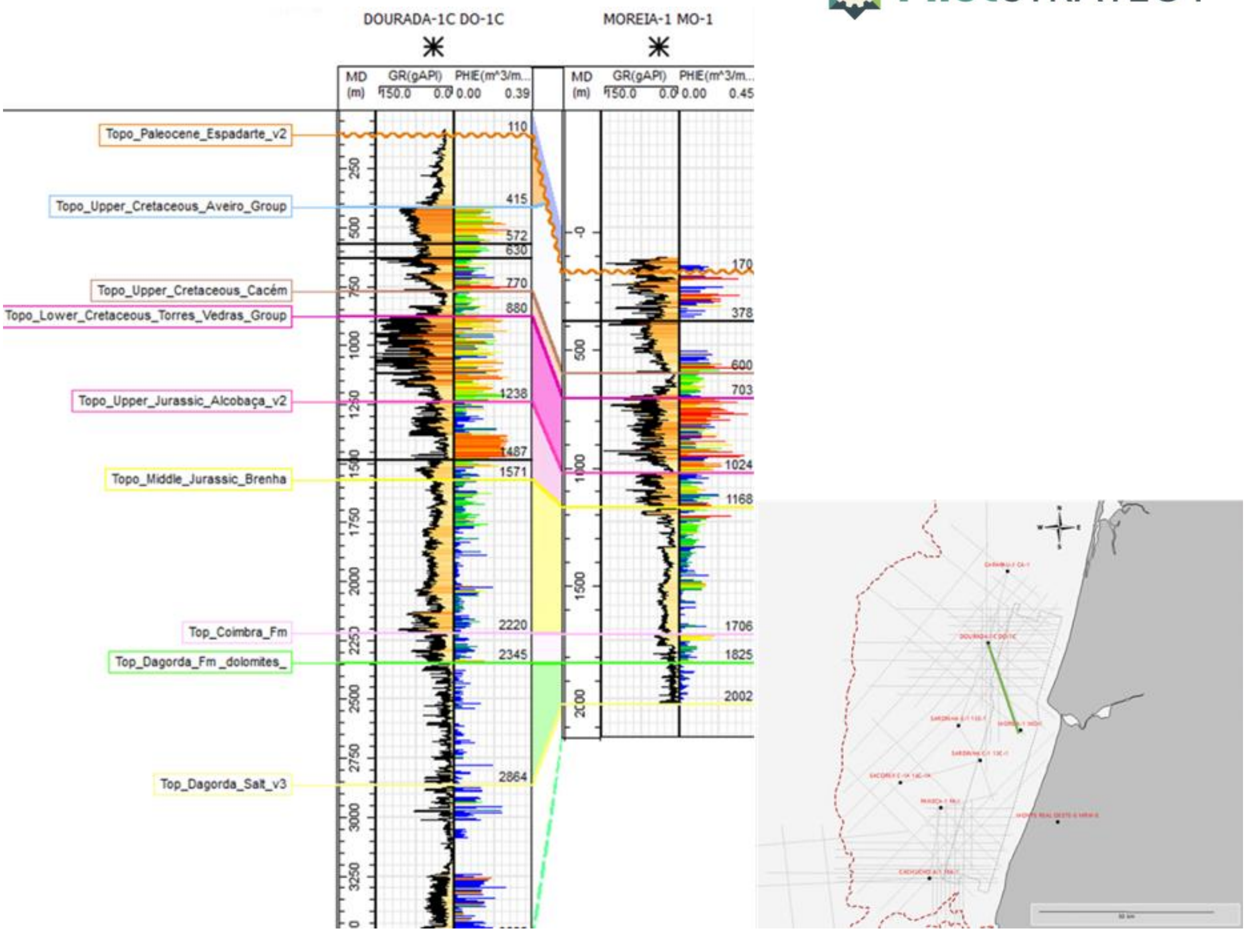

(b)

Figure 21: Well correlations crossing the a) Do-1C, 13C-1, Fa-1 and 16A-1 wells (N-S direction); and b) Do-1C and Mo-1 wells (NW-SE direction).

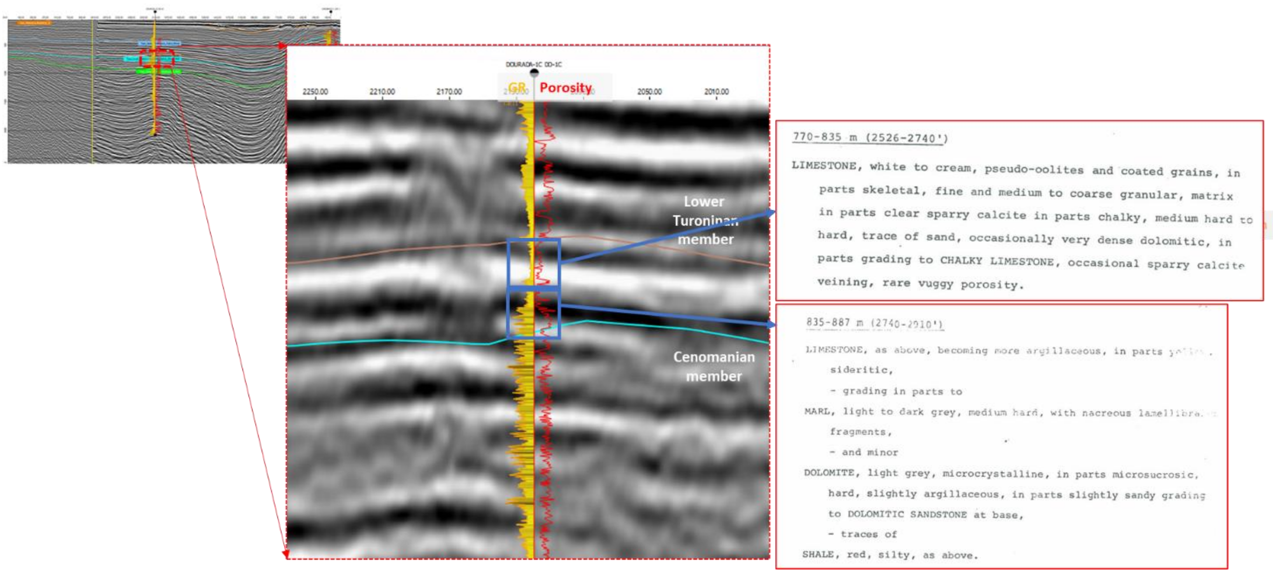

Figure 22: Seismic section focusing in the Cacém Formation and describing both upper and lower member lithologies of this sealing unit according to the report information from the Do-1C well.

The PilotSTRATEGY project has received funding from the European Union's Horizon 2020 research and innovation programme under grant agreement No. 101022664

4.5 Trap Characterization

The ranking and selection process of the identified closures suitable for carbon storage followed the application of scores and a set of technical criteria (e.g., storage and containment), which included the estimation of the expected capacity. Technical criteria to select potential structures as candidates for CO_2 storage was the presence of a structural component, such as 4-way, 3-way, or 2-way structural closures (these last two bounded by faults and/or salt diapir lithological contacts). After identifying several structures with potential size to serve as storage sites (Figure 23), we highlighted prospect Q4-TV1, preferentially oriented N-S, located in the northern study area, close to the Do-1C well. The characterization of this structure will be matured with the modelling studies that will take place in WP3 and WP4, particularly from the resulting static and dynamic reservoir models to confirm the evaluate the potential of this site for CO_2 storage.

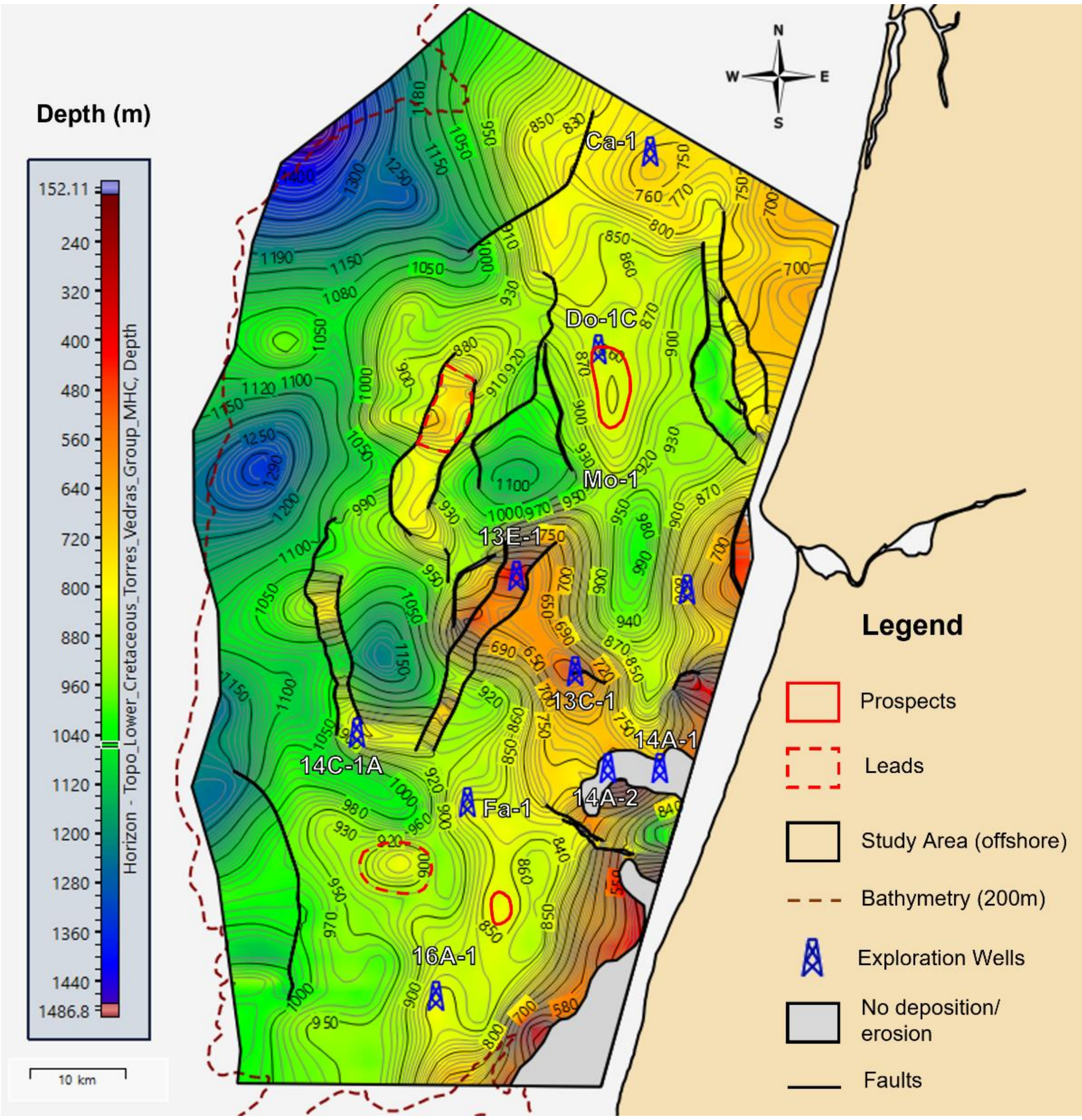

Figure 23: Location of four identified structural closures (basemap: Top Torres Vedras Group).

The PilotSTRATEGY project has received funding from the European Union's Horizon 2020 research and innovation programme under grant agreement No. 101022664

This structure lies in the northern flank of the broad anticlinal structure that was penetrated by the Do-1C well, and the trap type consists in a 4-way dip closure with a lateral extension of about 25 km^2 (in the P50 scenario). Despite the large extension of the prospect, its lateral closure is relatively flat and subtle, with a gross thickness of about 30 m.

Besides the definition of the P90 scenario, an alternative scenario of the structure's extent is given by the P10 outline (Figure 24), presenting a similar spatial orientation as the P50 scenario, but with a larger extent (250 km^2) and gross thickness of about 70 m. In this case, the trapping configuration is defined by a 2-way dip closure against N-S oriented faults, and the prospect is bounded to the south and northern areas by the lowest closing contour.

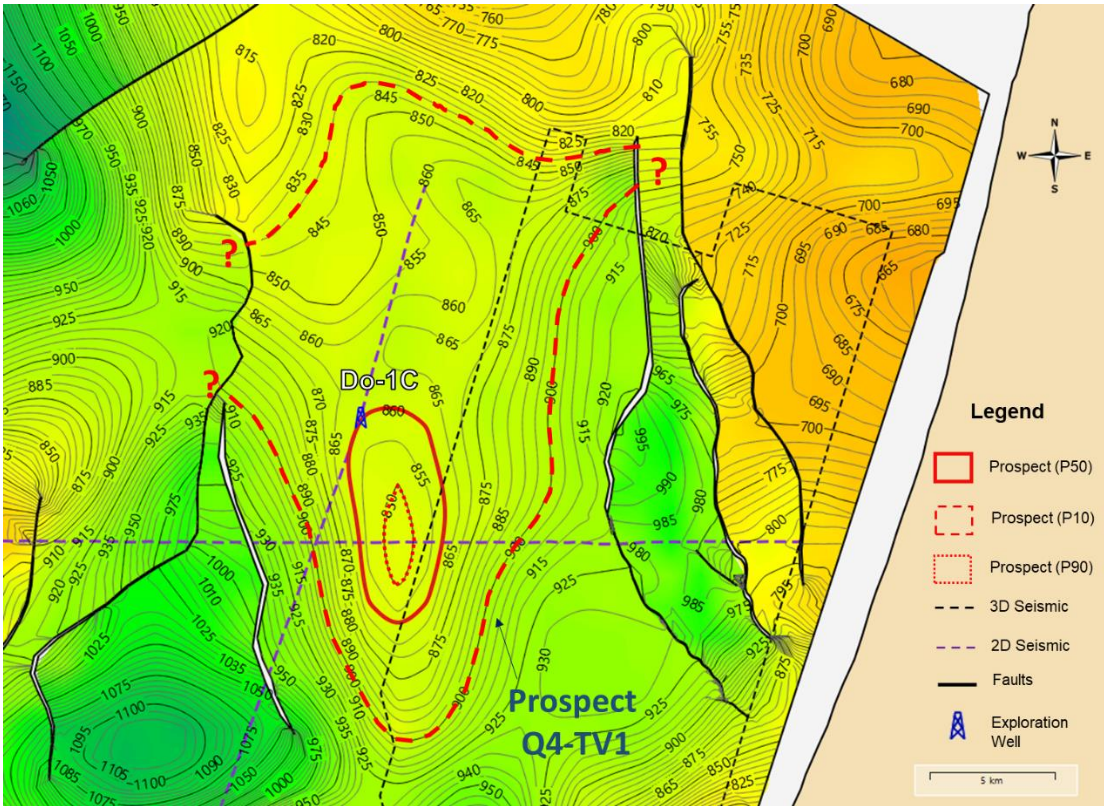

Figure 24: Location and outline definition of the Q4-TV1 prospect and P10-P50-P90 closures (red rectangles). The NE-SW and E-W 2D seismic sections (dashed purple lines) are illustrated in Figure 20 and Figure 25, respectively.

In addition to these structural closures in the north and south boundaries of the prospect, particularly evident in the southern part of the structure, according to the lithology information of the Ca-1 well, stratigraphic traps may also occur in the north of the prospect due to the lateral facies variation with reservoir thinning (and possible pinch-out). It is also important to mention that there is no information about the sealing conditions (i.e., permeability and transmissivity) of the faults closing the structure, so trap definition to the east and west must be accounted as a risk. Figure 25 shows an East-West interpreted seismic cross-section over the Q4-TV1 prospect, in which it is possible to observe the subtle anticline that defines the P50 outline, as well as the subvertical faults (some reaching out to the seabed) that define the P10 closure.

In general, and besides presenting better data quality and coverage, this promising storage site also presents higher scores of the technical criteria and the possibility of upside from a CO_2 storage pilot to a potential commercial scale. Subsurface results will directly feed the subsequent work packages

The PilotSTRATEGY project has received funding from the European Union's Horizon 2020 research and innovation programme under grant agreement No. 101022664

for the PilotSTRATEGY's LB study area, in which the team expects to mature the site characterization through the geological modelling, incorporating uncertainty assessments of structural and property models, followed by the dynamic reservoir simulation studies.

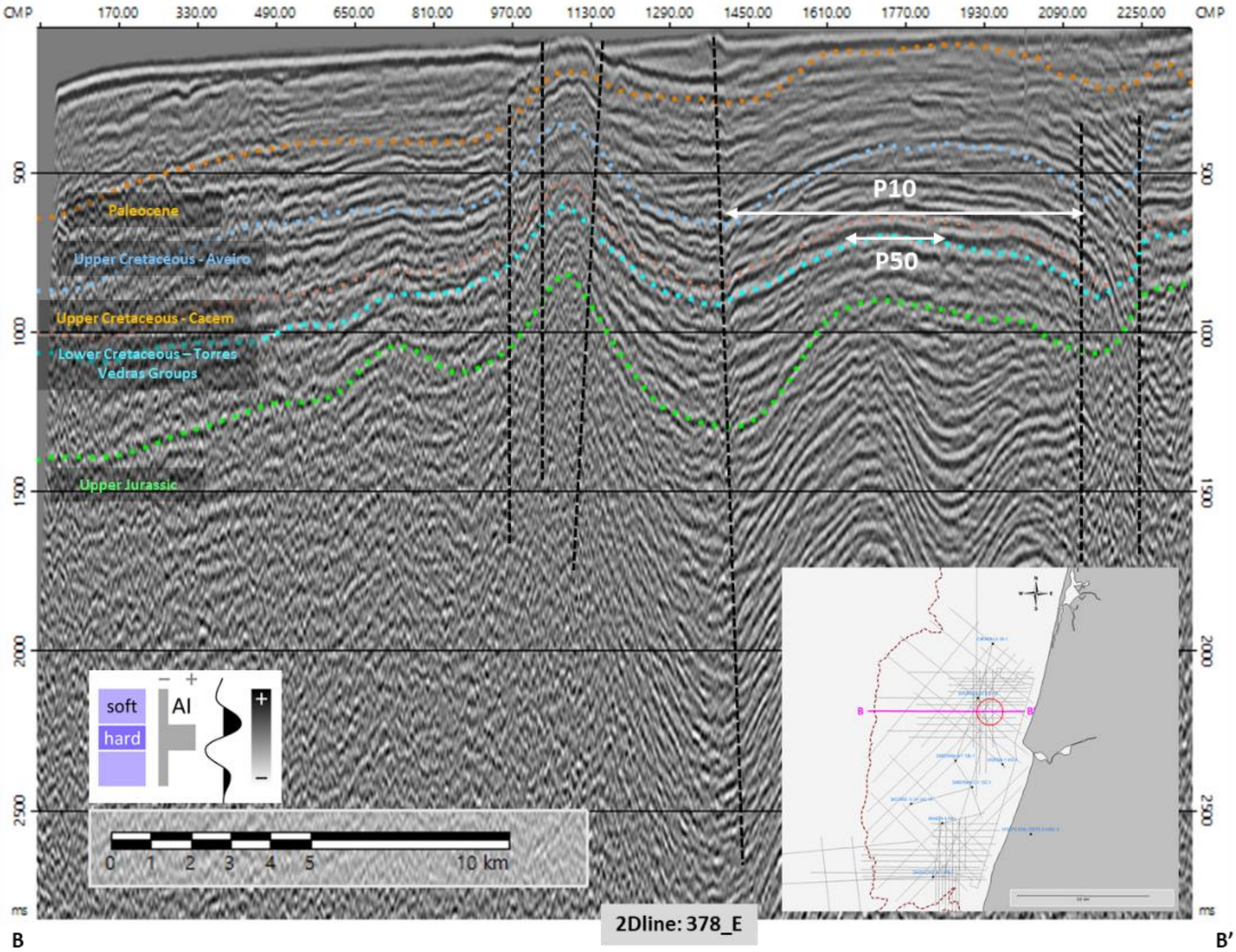

Figure 25: E-W seismic section crossing the selected prospect Q4-TV1 (highlighted in red) and illustrating the identification of P10 and P50 closures.

5. Facies analysis

5.1 Reservoir Facies

5.1.1 Stratigraphy

As crustal stretching progressed throughout the Early Cretaceous, a basin-ward migration of the rift locus was recorded (Murillas et al., 1990; Alves et al., 2009), mostly due to continental crust thinning and rupture in the Upper Barremian, followed by exhumation and thinning of the upper mantle until the Aptian-Albian boundary (Pinheiro et al., 1996). This later rift stage ultimately led to the lithospheric

The PilotSTRATEGY project has received funding from the European Union's Horizon 2020 research and innovation programme under grant agreement No. 101022664

breakup and the onset of seafloor spreading between the WIM and the Canadian Grand Banks since the Late Aptian (Pinheiro et al., 1996; Dinis et al., 2008).

This Early Cretaceous interval corresponds to deposition of shallow marine to fluvial sandstones in the Northern Lusitanian Basin, followed by an erosional event just before lithospheric breakup (paleoenvironmental maps that describe the evolution of this sedimentation phase are shown in Figure 26).

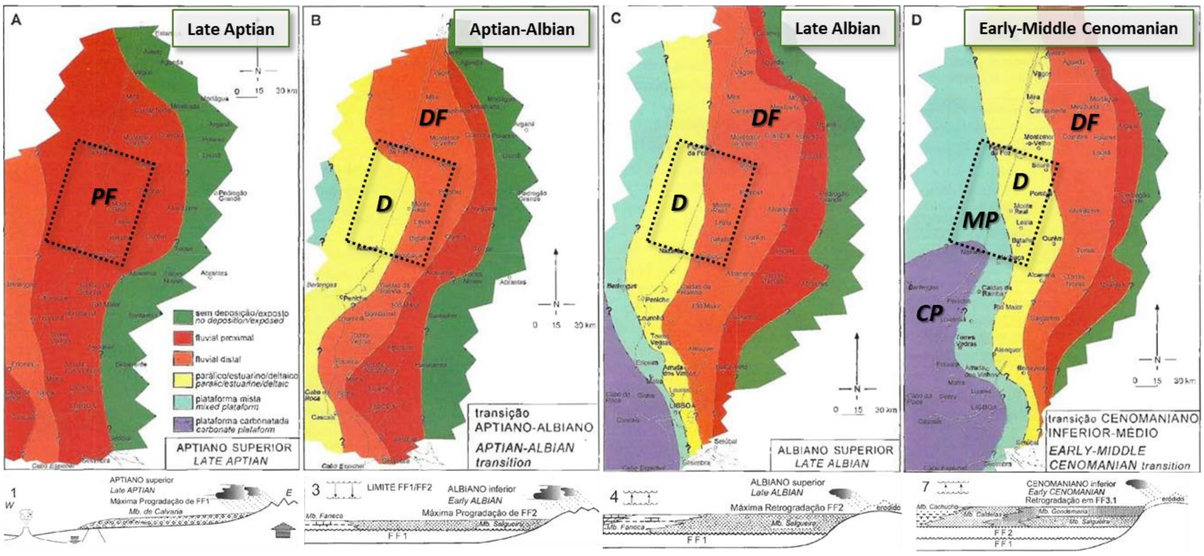

Figure 26: Paleogeographic reconstructions of the northern sector of the Lusitanian Basin from the Late Aptian to the Early-Middle Cenomanian (adapted from Rey et al., 2006). These sketches represent the depositional environments from the Torres Vedras Group (Late Albian) into the lower Cacém Formation (Early-Middle Cenomanian). DF – Distal Fluvial; D – Deltaic/Estuarine/Paralic; MP – Mixed Platform; CP – Carbonate Platform.

This siliciclastic interval is named specifically in the northern LB as the Figueira da Foz Formation but is commonly known in West Iberia as the TVG. As previously described, this is the main reservoir target considered for carbon storage in this study, mostly due to its very good porosity (no permeability data available) and hydrocarbon shows found in previous exploration campaigns and in nearby outcrops.

5.1.2 Reservoir Architecture

Some of the wells located on top of interpreted salt diapirs record a fair amount of the TVG interval. This can indicate that some diapirs should not have been present at the time of deposition, and probably have developed later, during the Miocene inversion phase. A map with interpreted salt diapirs embedded with the top TVG allows to show a generic correlation between structural highs and the presence of diapirs in the area (Figure 27).

The PilotSTRATEGY project has received funding from the European Union's Horizon 2020 research and innovation programme under grant agreement No. 101022664

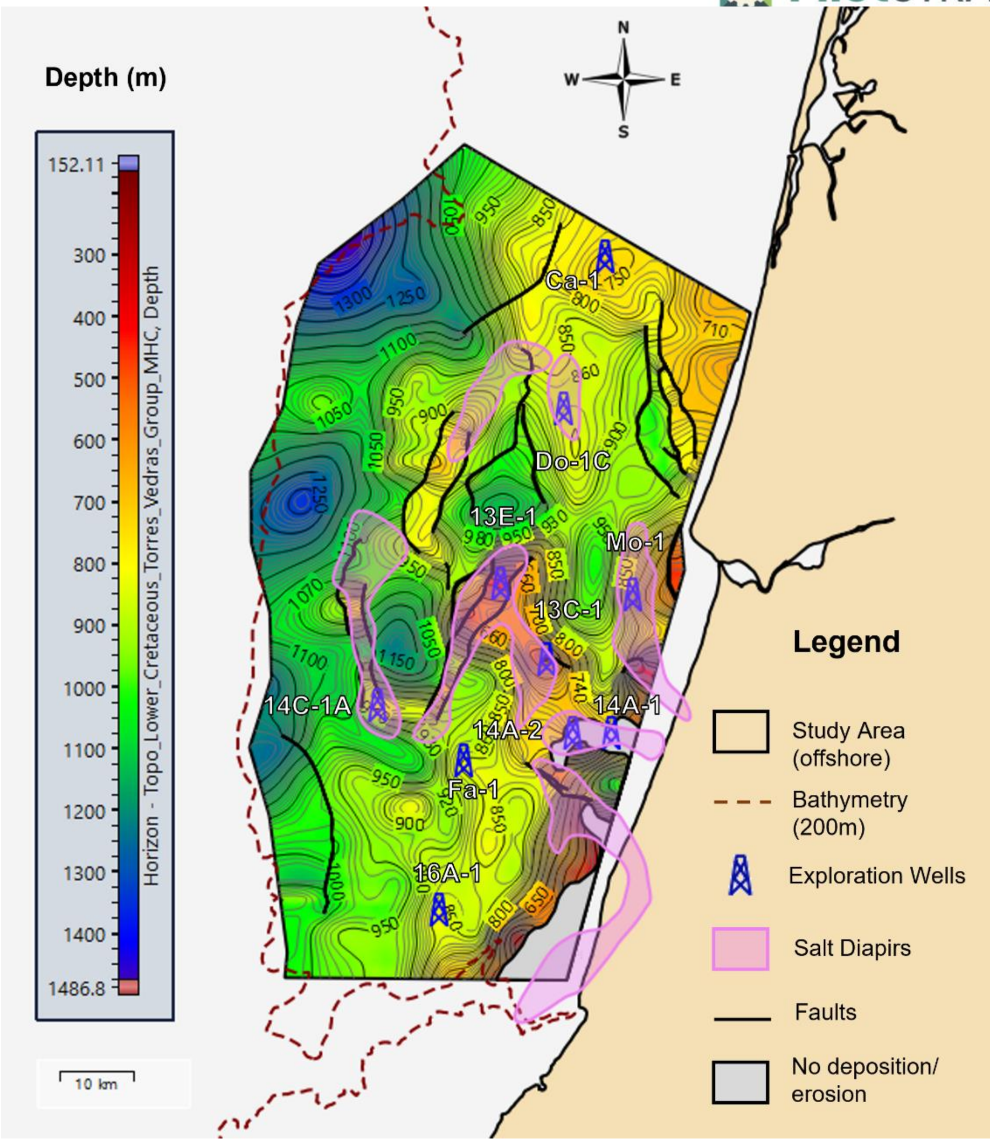

Figure 27: Map of the top Torres Vedras Group with interpreted faults and main salt diapir outlines.

A thickness map produced for the TVG (between Top Alcobaça Formation and Top TVG horizons) also gave valuable insights into sedimentary variations, as well as the impact of diapirism in defining sedimentary pathways and eventual bypassing (Figure 28).

The PilotSTRATEGY project has received funding from the European Union's Horizon 2020 research and innovation programme under grant agreement No. 101022664

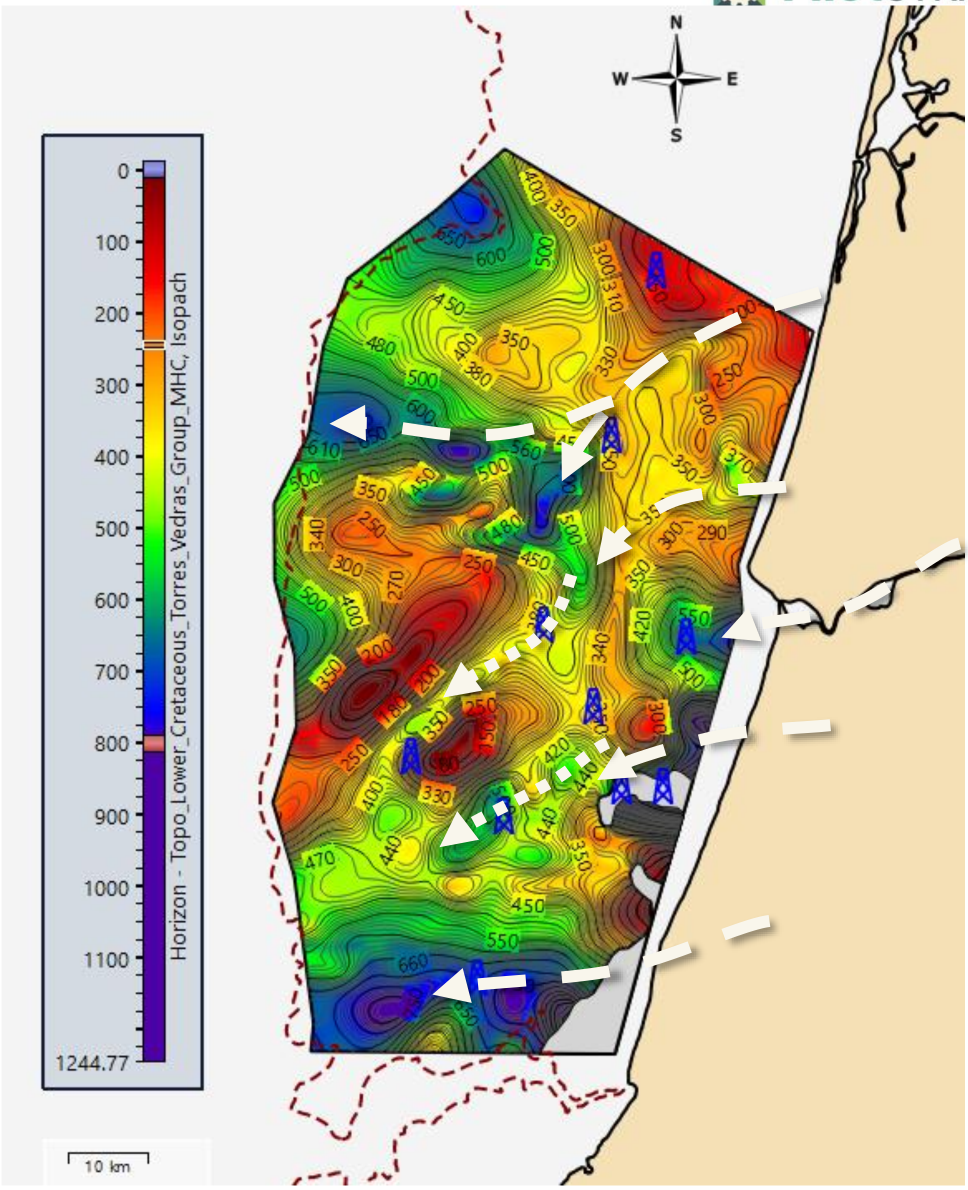

Figure 28: Isopach map (metres) of the Torres Vedras Group unit (from Top Alcobaça Formation to Top Torres Vedras Group), with possible sedimentary fairways.

The lack of good quality 2D and 3D seismic datasets made impossible to identify and interpret sandstone geobody continuity, as well as applying principles of sequence stratigraphy. Nevertheless, subsurface interpretation combined with the few existing public maps were able to generate an improved sketch of the depositional environment (Figure 29).

The map of Figure 29 also takes in account the total reservoir thickness found in each well, leading to the schematic drawing of the most likely sedimentary routes and bypass, as well as suggesting the presence of sub-basins locally created due to salt withdrawal. Despite presenting notable thickness, petrophysical interpretation in the wells show substantial claystone intercalations, probably reflecting the proximity to open marine sedimentation, and do not display the best reservoir facies in this area.

The PilotSTRATEGY project has received funding from the European Union's Horizon 2020 research and innovation programme under grant agreement No. 101022664

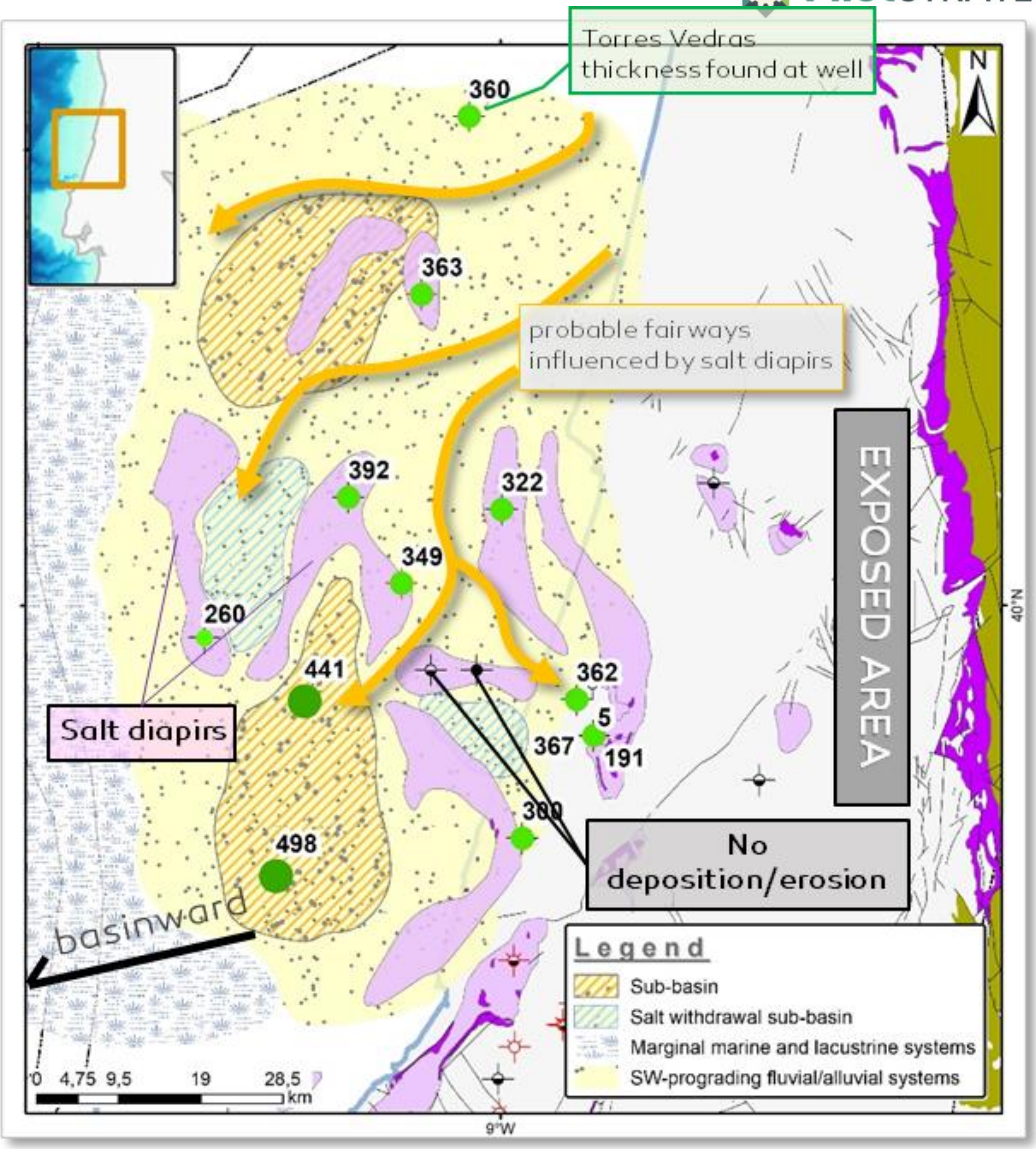

Figure 29: Paleoenvironmental sketch map at the Albian age (modified from Alves et al., 2002; Rey et al., 2006) that includes the interpreted sub-basins and salt diapirs in the study area, as well as the main sedimentary flow directions. Map also includes the indication of total thickness of Torres Vedras reservoir found in each well.

In the southwest portion of the study area, two wells (Fa-1, 16A-1) show particularly thick intervals (441 to 498 meters), in a basin-ward area where no salt diapirs are interpreted. This map also allows to show the relationship between salt diapirism, timing of emplacement, and sedimentation during the Early Cretaceous. Despite generally observing 300 to 500 meters of gross thickness, it is also possible to observe the absence of the Torres Vedras unit in the Espadarte wells (14A-1, 14A-2), and negligible in MRW-5 (drilled onshore). This can be interpreted as the result of salt ascent and erosion during the Miocene tectonic inversion phase, which acted locally, as indicated by strong thickness variations (sometimes hundreds of meters) in wells located close by.

The PilotSTRATEGY project has received funding from the European Union's Horizon 2020 research and innovation programme under grant agreement No. 101022664

5.1.3 Reservoir Properties

Cretaceous reservoir rocks are sandstones of variable grain size and sorting. Sandstone cements are often of carbonate nature, although siliceous, clay-rich and ferruginous cements are also common.

Reservoir samples are sandstones, with variable grain sizes, ranging from fine to coarse-grained sandstones with variable sorting. The grains are mainly quartz, although feldspar grains and lithoclasts are often found. Most of the samples have a calcitic cement; siliceous cement, kaolinite rich cement and iron oxy/hydroxides cement are also common. Types of cement tend to be heterogeneously distributed both laterally and vertically through the reservoir rocks. Quartz is the main mineralogical constituent, orthoclase, magnesian calcite, kaolinite, microcline, dolomite and micas are also common constituents of the sandstones.

The detrital sedimentation, related to the rifting episodes of the LB, started during the Late Jurassic. The thick sandstone reservoir sequence also includes, in some sectors of the basin, the Upper Jurassic sediments. These sediments were also sampled (although not foreseen in the initial proposal) and are medium- to coarse-grained sandstones, poorly sorted with sub-angular grains (very similar to the Cretaceous samples) with a carbonate cement.

The map of Figure 30 shows the sampling locations performed in the LB for the TVG reservoir unit and for the CF seal unit. Geomechanical and geochemical laboratorial results are synthetized in this sub-chapter and in the following sub-chapter that refers to seal properties.

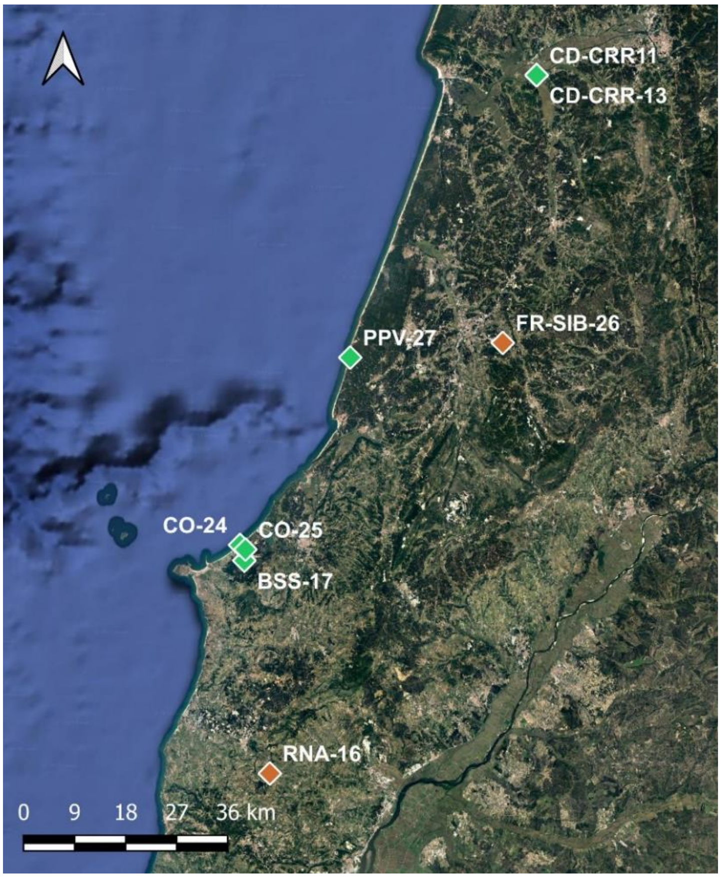

Figure 30: Sample locations of the Torres Vedras Group reservoir unit (green symbol) and Cacém seal unit (orange symbol).

The PilotSTRATEGY project has received funding from the European Union's Horizon 2020 research and innovation programme under grant agreement No. 101022664

Laboratorial geomechanical analysis on the TVG reservoir was not possible due to the low sample consolidation. Only data on the seal and on the Upper Jurassic reservoir is available. The Upper Jurassic sandstones have dynamic elastic modulus averaging between 16.79 GPa (perpendicular to the anisotropy – bedding) and 29.29 GPa (parallel to the anisotropy). Tensile strength has an average value of 0.32 MPa while the uniaxial compressive strength averages 7.71 GPa. The sample has an elasticity modulus of 5.50 GPa. The Cretaceous seal (CF) presents an average dynamic elastic modulus of 2.55 GPa. Tensile strength has an average value of 1.08 MPa while the uniaxial compressive strength averages 30.05 GPa. The elasticity modulus of the seal averages 17.28 GPa.

Petrophysical data on the outcrop samples (performed at IFPEN) can be synthesized as follows:

i) porosity values determined through mercury injection and Helium porosity for the Upper Jurassic reservoir range between 10.0 and 10.5 %, while porosity values from NMR range between 11.3 and 12%;
ii) water permeability (NMR) averages 0.10 mD;
iii) Formation factor values fluctuate between 75.5 and 96.5;
iv) Water saturation after air-brine centrifuge at 7 bar averages 0.53;
v) Clay bound water averages 0.54.

Thermal conductivity, volumetric thermal capacity, and thermal diffusion were also determined for the samples: a) thermal conductivity for the Upper Jurassic reservoir samples have an average of 2.59 W/mk (minimum of 2.07 W/mk, maximum of 3.14 W/mk); b) volumetric thermal capacity ranges between 1.38 and 2.30 (J/m³,K) x10^6 with an average of 2.59 (J/m³,K) x10^6 and; c) thermal diffusion averages 1.53 (m²/s) x10^{-6} ranging between 1.05 and 1.97 (m²/s) x10^{-6}.

Mineralogical characterization of the samples collected at the different outcrops was performed through X-ray diffraction and thermo-gravimetric analysis. The results of semi-quantitative determination of mineral percentages from XRD and TGA are presented in the

Table 5.

Table 5: Mineralogical analysis of the collected Torres Vedras reservoir samples.

	XRD				
	Quartz	K-felspar	Calcite	Kaolinite	Micas
CD-CRR-10	44.1	55.9	-	-	-
CD-CRR-11	85.3	14.7	-	-	-
CD-CRR-12	95.4	4.6	-	-	-
CD-CRR-13	97.0	3.0	-	-	-
BSS-17	95.9	-	-	4.1	-
BSS-17 *	15.0	-	-	75.0	10.0
BSS-18	30.0	-	-	17.5	47.5
BSS-18 *	28.9	-	-	37.0	34.1

The PilotSTRATEGY project has received funding from the European Union's Horizon 2020 research and innovation programme under grant agreement No. 101022664

5.2 Seal Facies

5.2.1 Stratigraphy

The Albian to Cenomanian/Turonian lithospheric breakup sequence is recognized in the LB, reflecting fluvial deposits (Wilson et al., 1989; Rey et al., 2006; Dinis et al., 2008) capped by shallow-marine carbonates associated with a Cenomanian-Turonian transgression (Witt, 1977) (Figure 31).

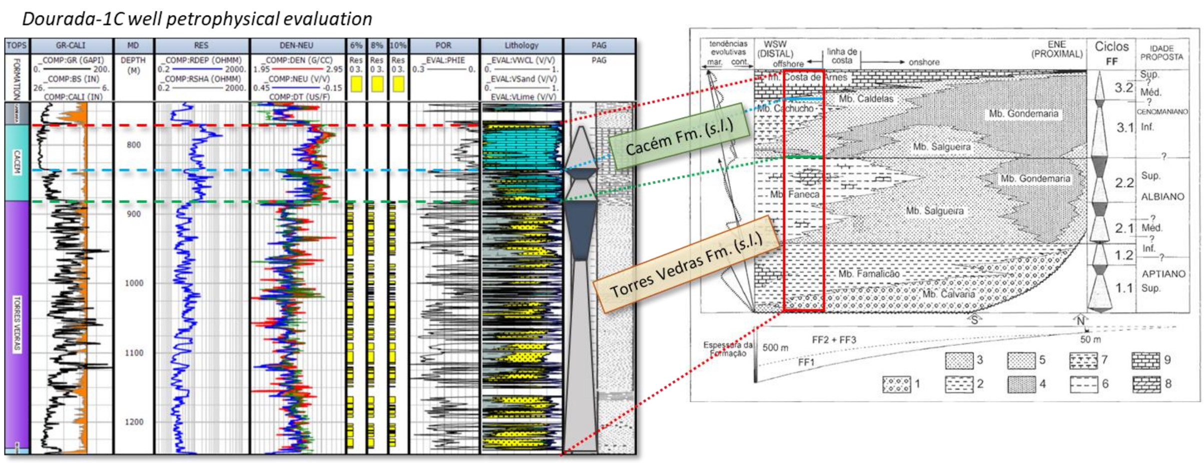

Figure 31: Correlation between the petrophysical analysis for Do-1C well and the onshore stratigraphical record (Rey et al., 2006), focused on the transition between the Torres Vedras Group (which here presents very good porosity sandstones) and the Cacém Formation. A notable correspondence can be seen between Transgression-Regression cycles and the subdivision of the Cacém Formation into a shaly lower member and a dolomitic/carbonate upper member.

This carbonate-rich unit is a very continuous and relatively thin interval (less than 200m) that is widely recognized in seismic datasets across WIM as a double-loop reflector (Figure 25), corresponding to the CF sealing unit. It is typically composed by two sub-units, in which the Lower CF consists of a thin shale/marl package (<50m), followed by the Upper CF, with 50 m to 100 m of limestone and/or dolomite. These lithologies can often be weathered, resulting in reddish-grey sediments that are likely to result from subaerial exposure and mild karstification, although no geological hints were identified in the study area to justify this.

5.2.2 Seal Properties

Cretaceous primary seal is mainly constituted by carbonate rocks. Limestone and dolomite are the most common lithologies, although some claystone and interbedded thin layers of sandstone are present in the primary seal formation. Seal lithotypes collect at the outcrops have diverse textural characteristics that can be summarized as follows: i) wackestone with abundant bioclasts of gastropod and lamellibranch with calcite as the solely mineralogical component; ii) dolomite with minor amounts of detrital quartz and K-felspar and diagenetic calcite; iii) micritic limestone (only calcite was revealed by the X-ray diffraction) with bioclasts and profuse stylolithic surfaces, frequently open in the collected samples; iv) microsparitic limestone with abundant bioclasts and some intraclasts and quartz grains dispersed throughout the sample.

Thermal conductivity, volumetric thermal capacity, and thermal diffusion were also determined for the CF seal samples: a) thermal conductivity has an average of 2.39 W/mk (minimum of 1.68 W/mk,

The PilotSTRATEGY project has received funding from the European Union's Horizon 2020 research and innovation programme under grant agreement No. 101022664

maximum of 3.59 W/mk); b) volumetric thermal capacity ranges between 1.74 and 2.67 (J/m^3,K) x10^6 with an average of 2.10 (J/m^3,K) x10^6 and; c) thermal diffusion averages 1.11 (m^2/s) x10^{-6} ranging between 0.83 and 1.55 (m^2/s) x10^{-6}.

Mineralogical characterization of the samples collected at the different outcrops was done through X-ray diffraction and thermo-gravimetric analysis. The results of semi-quantitative determination of mineral percentages from XRD and TGA are presented in Table 6.

Table 6: Mineralogical analysis of the collected Cacém Formation seal samples.

	XRD					TGA
	Quartz	K-feldspar	Calcite	Kaolinite	Micas	
CD-DARN-14	60.6	23.5	15.9	-	-	30.8 cal
CD-DARN-15	6.9	9.8	83.3	-	-	90.0 cal
RNA-16	-	-	100	-	-	98.1 cal

After applying a cut-off (<2% Phie), seal net-thickness was estimated for each well in the study area (Table 7), on top of an isochore map for the CF.

Table 7: Summary of seal properties estimated from petrophysical analysis for the Cacém Formation and the Aveiro Group.

	Cacém Formation (PHIE < 2%)							Aveiro Group (PHIE < 2%)				
Well Name	Top (MD m)	Bottom (MD m)		Gross (m)	Net (m)		N/G (%)	Top (MD m)	Bottom (MD m)	Gross (m)	Net (m)	N/G (%)
Do-1C	770	880		110	14.33		13%	630	770	140	20.57	15%
Mo-1	**600**	**703**	103	10.82	11%	378	600	222	173.76	78%		
13C-1	**303**	**412**	109	16.61	15%	227	303	76	-	-		
13E-1	**245**	**356**	111	37.78	34%	-	-	-	-	-		
14C-1A	**693**	**782**	89	45.87	52%	465	693	228	166.99	73%		
Fa-1	738	860	122	39.17	32%	450	738	288	44.2	15%		
16A-1	858	974	116	19.96	17%	673	858	185	8.53	5%		

Due to lack of quality of the available 3D seismic dataset and the uniform and continuous character of the CF seismic reflectors, it was not possible to address the seal property study into detail using seismic attributes or applying principles of sequence stratigraphy to seismic datasets.

In addition to the petrophysical and laboratorial analysis, following a visit to the national repository of well data, we conducted a study based on a macroscopic analysis on well cuttings and cutting

The PilotSTRATEGY project has received funding from the European Union's Horizon 2020 research and innovation programme under grant agreement No. 101022664

descriptions contained in well reports. To better characterize the sealing quality from macroscopic analysis, we subdivided this into three separate categories that include:

1) Unweathered limestones, dolomites and/or shales;

2) Semi-altered heterogeneous lithologies (limestones and/or shale);

3) Weathered limestones or dolomites.

This resulted in a conceptual traffic-light sketch (Figure 32) that helps to understand where the best seal facies in the study area can be found, per well, supporting the decision to choose the area that encompasses the Do-1C and 13E-1 wells as the less risky to find better preserved seal.

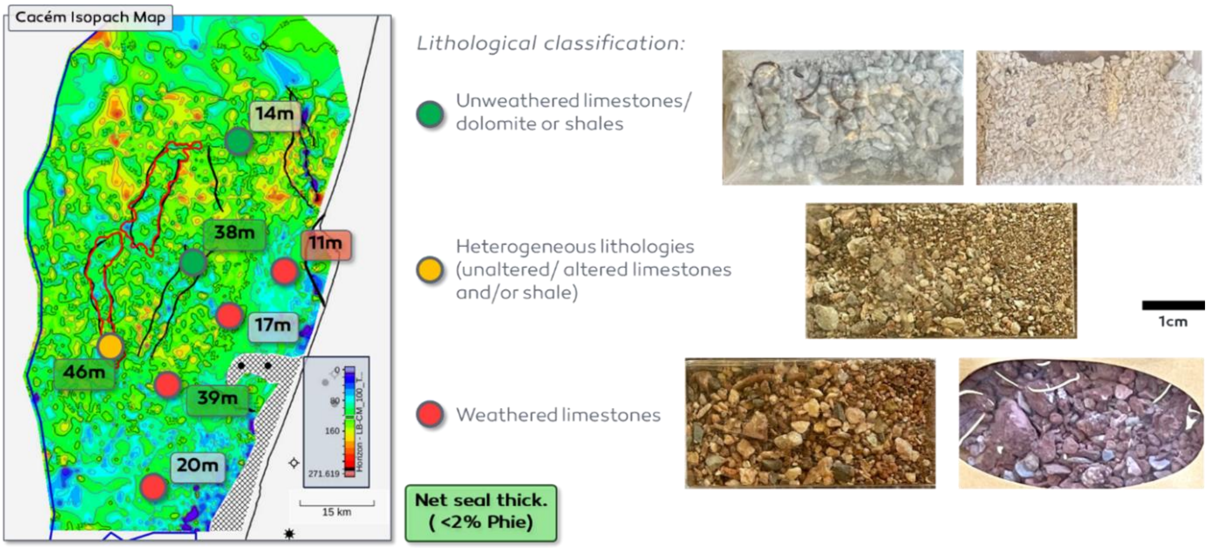

Figure 32: Lithological classification made after macroscopic analysis of well cuttings for the Cacém Formation interval penetrated by wells in the study area. Cacém isopach map contains the traffic-light graphical representation of the quality of seal lithologies. Adjacent to each well location there is the indication of the seal net-thickness, as estimated through petrophysical log analysis (see criteria on Table 7).

Do-1 and 13E-1 wells show the best seal facies of the whole seven wells in the region, with the presence of unweathered limestones/dolomites and shales, which may be locally explained due to the combination of lack of syn-diapirism deposition (with rapid deposition with no subaerial exposure), and no fracturing and/or folding during the tectonic inversion phases.

One additional aspect used to address the overburden (combined by the CF, the Aveiro Group and the Cenozoic strata) was a thickness variation map (Figure 33).

The PilotSTRATEGY project has received funding from the European Union's Horizon 2020 research and innovation programme under grant agreement No. 101022664

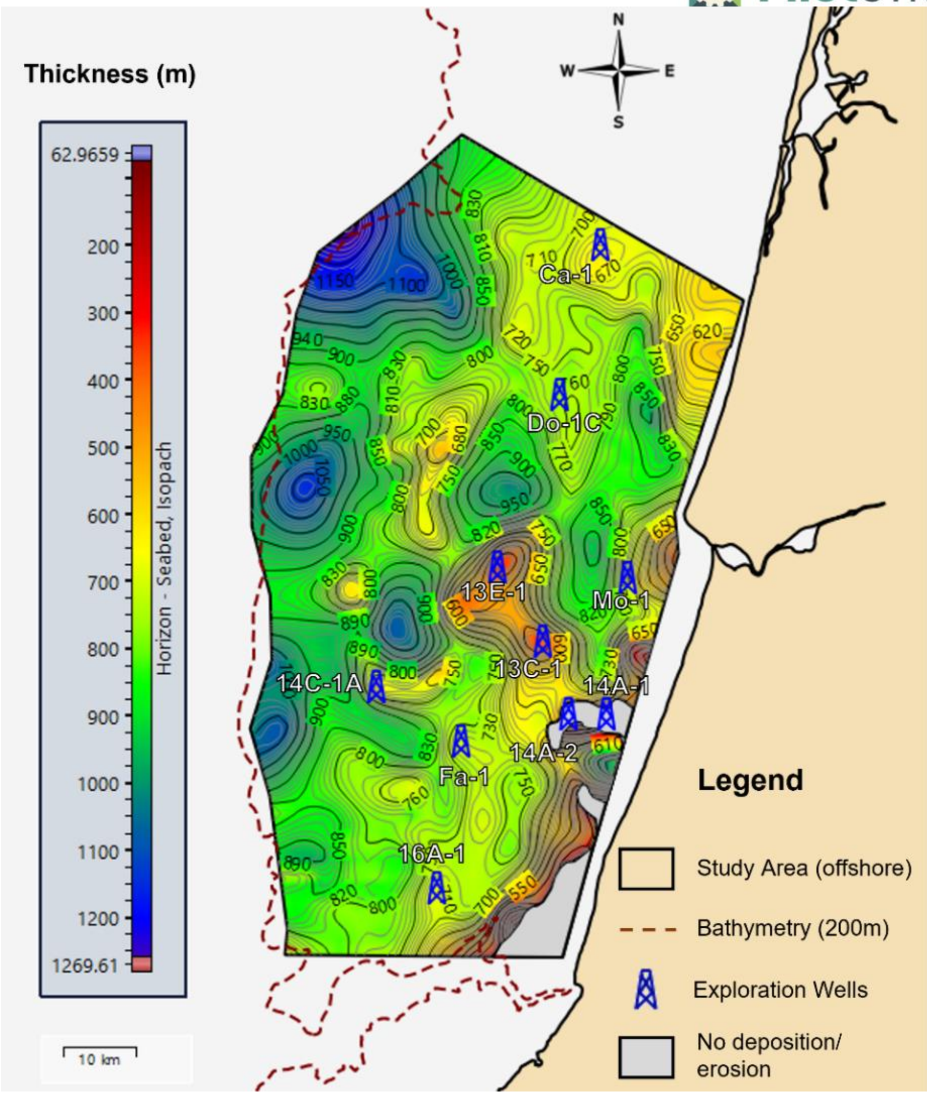

Figure 33: Isopach map (metres) produced from the top of the Torres Vedras reservoir unit until seabed. It can be observed a thin overburden over the area covered by the 13E-1 and 13C-1 (Sardinha) wells, as well as to the east. Overall, the study area presents reasonable thickness values (~650m to >1100m).

The overburden thickness map generically shows a thickening trend from east to west, towards the present-day continental shelf-break (200m bathymetric isoline). It is also noticeable several places with thin strata dispersed across the study area, associated with punctual salt diapirism. Apart from these locations, the average estimated overburden of ~650m to >1100 m associated with the regional geothermal gradient (~30ºC/km) suggests there is conditions to preserve CO_2 in a supercritical phase.

6. Surface Data

As the selected study area in focused offshore, there is little information that could be used for geological characterization apart from well and geophysical data. However, there are outcrop analogues of the TVG reservoir, in which several depositional patterns typical of fluvial-deltaic-shoreline environments can be observed (e.g., Praia d'el Rey). Some of these include well-rounded, well sorted, quartz-rich sandstones within channel deposits, delta-front/mouth bar deposits, as well as distributary-channels and interbedded floodplain silts and claystones. The lithological complexity,

The PilotSTRATEGY project has received funding from the European Union's Horizon 2020 research and innovation programme under grant agreement No. 101022664

interbedding and thickness variations generally found in wells and in seismic data is also perceived, in a smaller scale, in outcrops (Figure 34 and Figure 35).

Figure 34: Sedimentary patterns of the Torres Vedras Group (location: Pedras d'el Rey beach).

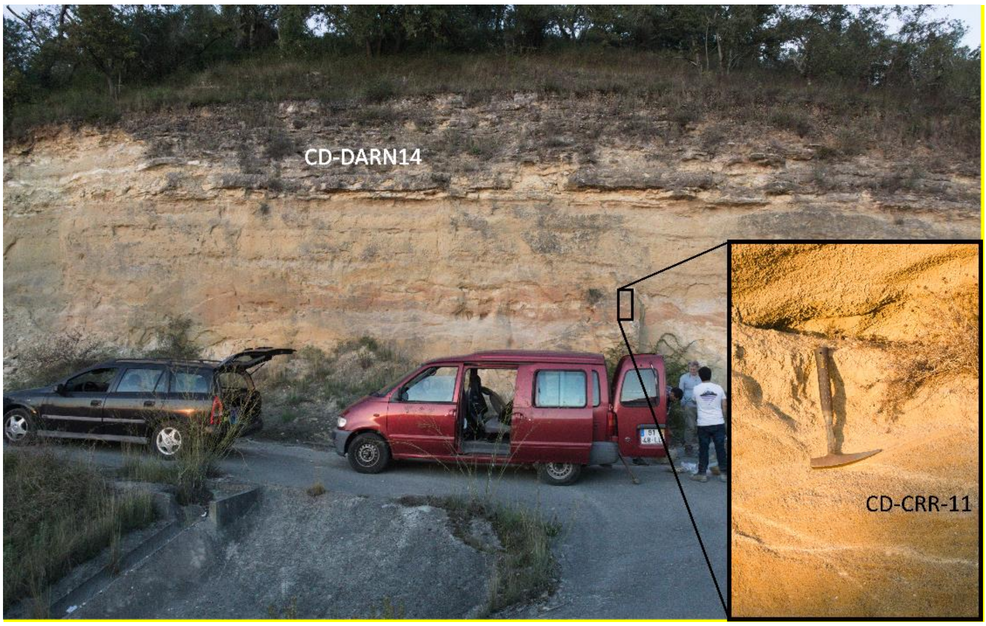

Figure 35: Outcrop of the transition from the Torres Vedras Group (reservoir) to the Cacém Formation (seal), from which some of the samples were taken (Easting: 528022.32; Northing: 4444780.84).

These variations reflect the interplay between sedimentary load, eustasy, as well as the structural control of existing sub-basins and salt diapirs. They also attest the difficulty to map in detail the several reservoir packages at a larger scale. Most of these lithological variations, intercalations, and lateral facies changes do not display the proper seismic resolution to be distinguished, so this detailed analysis was not considered in this assessment. Figure 39 shows one of the locations where sampling was performed, and where the lithological transition from the sandy Upper TVG unit to the shaly/marly Lower Member of the CF can be clearly identified.

The PilotSTRATEGY project has received funding from the European Union's Horizon 2020 research and innovation programme under grant agreement No. 101022664

7. Depositional Environments and Geological Conceptual Model

As a conclusion, the storage complex selected for modelling purposes in WP3 is composed by:

- Primary seal – CF is a thick sealing layer conformably sitting on top of the reservoir in the Upper Cretaceous, which combines in the topmost part limestone and dolomite, deposited in a marine carbonate platform, and marls and clays at the base. Salt diapirism does not impact the deposition of CF carbonates (as it can be seen by the relatively uniform thickness maps on Figure 36 and Figure 37)
- Main reservoir – The main storage potential is identified in the Lower Cretaceous section, denominated as the TVG. This formation is mainly composed by Late Aptian – Cenomanian sandstones, deposited in a fluvial environment with interbedded sealing clays that have been observed and described in some nearby wells. The sedimentary fairways are influenced by salt tectonics and, based on existing wells, reservoir depths are between 500m to 1000m. The TVG shows good reservoir properties, and the trapping mechanism can be described as structural/stratigraphic (Figure 36, Figure 37)
-

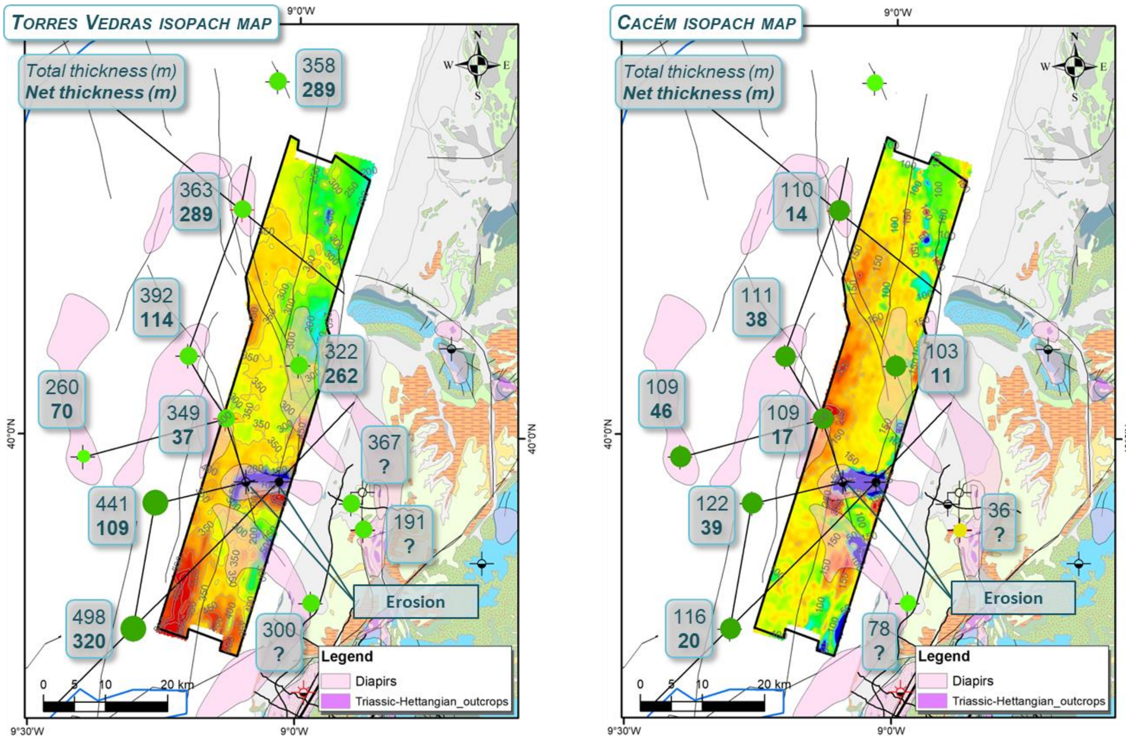

(a) (b)

Figure 36: Isopach maps and thickness for the (a) Torres Vedras Group and the (b)Cacém Formation.

The PilotSTRATEGY project has received funding from the European Union's Horizon 2020 research and innovation programme under grant agreement No. 101022664

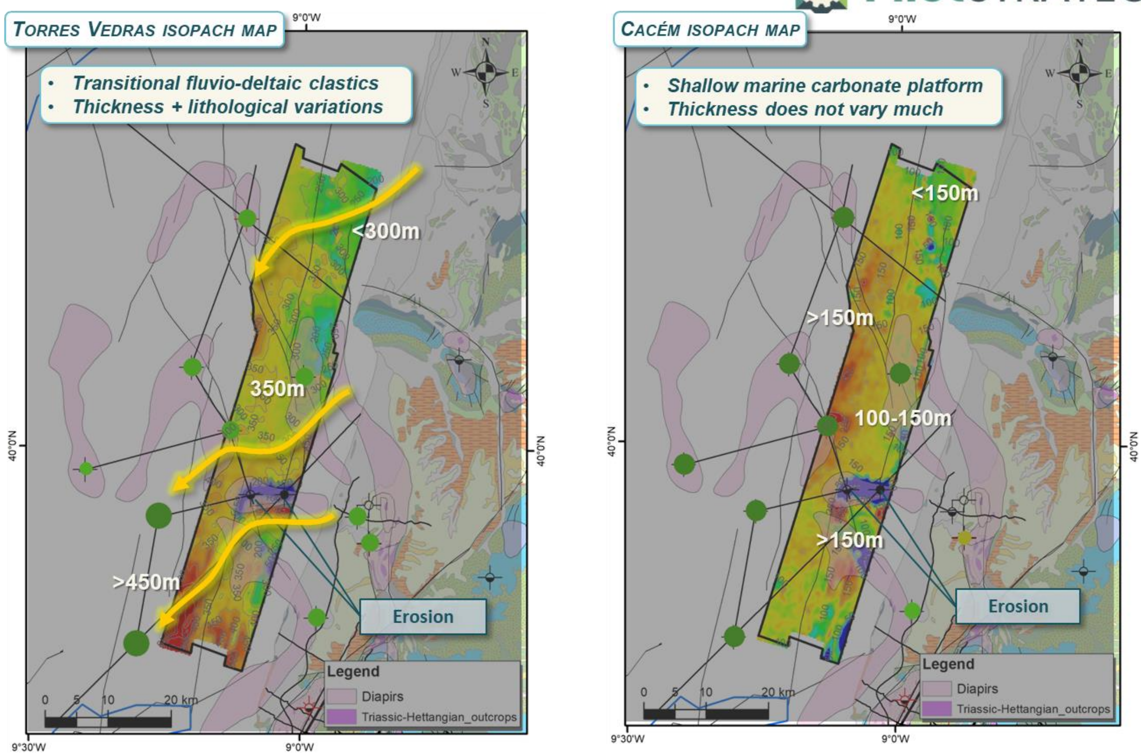

Figure 37: Simplified sedimentary fairways for the (a) Torres Vedras Group; (b) the Cacém Formation consists of a carbonate platform with no significant thickness differences.

- Potential Secondary Reservoir

An additional potential reservoir can be considered in the Upper Jurassic (Alcobaça Formation), with reasonably good reservoir characteristics of alternating sands and marls, as well as limestones deposited in shallow carbonate platform/ transitional environments.

- Overburden

The main units that composed the overburden (Late Cretaceous and Cenozoic sediments) and will be part of the static model are 1) the Espadarte Formation, which is composed by dolomites and an alternation of clay and fine-coarse sandstones, deposited in a fluvial/lacustrine marine environment (Pereira et al., 2022); and 2) the Aveiro Group, which is a potential secondary seal composed by alternating sands and claystones.

- Underburden

The main units below the storage complex are two members of the Brenha Group, which consist of 1) Brenha Formation (s.s.), a succession of dolomites and dolomitic limestones (Coimbra Formation); and limestones intercalated with centimetric layers of marls, in the upper section; and 2) the Dagorda Formation, which represents the top of the salt unit and is mainly composed by evaporitic strata. Although the underburden area is not relevant for the dynamic reservoir simulations of fluid flow, the static model will incorporate the adjacent unit underneath the main reservoir (Alcobaça and Brenha formations) for the geomechanical modelling purposes needed in the storage complex integrity studies of WP3.

The PilotSTRATEGY project has received funding from the European Union's Horizon 2020 research and innovation programme under grant agreement No. 101022664

8. References

Alves, T., Cunha, T.A., 2018 – A phase of transient subsidence, sediment bypass and deposition of regressive–transgressive cycles during the breakup of Iberia and Newfoundland. Earth and Planetary Science Letters, 484, p. 168–183

Alves, T., Gawthorpe, R.L., Hunt, D.H., & Monteiro, J.H., 2003 – Cenozoic tectono-sedimentary evolution of the western Iberian margin, Mar. Geol., 195, p. 75–108

Alves, T., Gawthorpe, R.L., Hunt, D.W., & Monteiro, J.H., 2002 – Jurassic tectono-sedimentary evolution of the Northern Lusitanian Basin (offshore Portugal). Marine and Petroleum Geology, 19, p. 727-754

Alves, T., Moita, C., Cunha, T., Ullnaess, M., Myklebust, R., Monteiro, J.H., and Manuppella, G., 2009 – Diachronous evolution of Late Jurassic-Cretaceous continental rifting in the northeast Atlantic (west Iberian margin). Tectonics, 28, TC4003, doi:10.1029/2008TC002337

Azerêdo, A.C., Duarte, L.V., Henriques, M.H., & Manuppella, G., 2003 – Da dinâmica continental no Triásico aos mares do Jurássico Inferior e Médio. Cadern. Geol. Portugal, Instituto Geológico e Mineiro, Lisboa, 43 p.

Baranov, V., & Naudy, H., 1964 – Numerical calculation of the formula of reduction to the magnetic pole. Geophysics, 29(1), 67-79.

Benjumea, B., Garcia-Crespo, J., Mediato, J.F., Rey-Moral, C., Ayala, C., Rubio, F., Soto, R., Clariana, P., Pueyo, E.L., Fernández-Canteli, P., 2022 - Passive Seismic Methods as Support for the Interpretation of Legacy Seismic Profiles: CO_2 Storage, 83rd EAGE Annual Conference & Exhibition; 2022 https://doi.org/10.3997/2214-4609.202210533

Casacão, J., Silva, F., Rocha, J., Almeida, J. and Santos, M., 2023 – Aspects of salt diapirism and structural evolution of Mesozoic–Cenozoic basins at the West Iberian margin. *AAPG Bulletin*, Volume 107(1), pp. 49–85. https://doi.org/10.1306/08072221100

Davison, I. & Barreto, P., 2020 – Deformation and sedimentation processes, and hydrocarbon accumulations on upturned salt diapir flanks in the Lusitanian Basin, Portugal. Petroleum Geoscience, 27, p. 138

Dinis, J.L., Rey, J., Cunha, P.P., Callapez, P., and Pena dos Reis, R., 2008 – Stratigraphy and allogenic controls of the western Portugal Cretaceous: an updated synthesis. Cretaceous Research, v. 29 (5-6), p. 772-780

Gunn, P. J., Fitzgerald, D., Yassi, N., & Dart, P., 1997 – New algorithms for visually enhancing airborne geophysical data. Exploration Geophysics, 28(2), 220-224.

Isles, D. J., & Rankin, L. R., 2013 – Geological interpretation of aeromagnetic data. Society of Exploration Geophysicists and Australian Society of Exploration Geophysicists.

Kullberg, J. C., Rocha, R. B., Soares, A. F., Rey, J., Terrinha, P., Azerêdo, A.C., Callapez, P., Duarte, L. V., Kullberg, M. C., Martins, L., Miranda, R., Alves, C., Mata, J., Madeira, J., Mateus, O., Moreira, M. & Nogueira, C. R., 2013 – A Bacia Lusitaniana: Estratigrafia, Paleogeografia e Tectónica. In: Dias, R.,

The PilotSTRATEGY project has received funding from the European Union's Horizon 2020 research and innovation programme under grant agreement No. 101022664

Araújo, A., Terrinha, P. & Kullberg, J. C. (eds.) Geologia de Portugal. Lisboa: Escolar Editora, 2, p. 317-368

Leinfelder, R. R. & Wilson, R. C. L., 1998 – Third-order sequences in an Upper Jurassic rift-related second-order sequence, central Lusitanian Basin, Portugal. P. C. Graciansky, J. Hardenbol, T. Jacquin, P. R. Vail, SEPM Special Publication, 60, p. 507-525

Li, X., 2006 – Understanding 3D analytic signal amplitude. Geophysics, 71(2), L13-L16.

Lumley, D., Shragge, J., Issa, N, Kamei, R., Potter, T., Miyoshi, T., Pevzner, R., Bona, A., Tertyshnikov, K., Langhi, L., Sarout, J., 2014 – Feasibility and design of robust passive seismic monitoring arrays for CO_2 geosequestration, ANLEC Project 7-0212-0203

Maxwell. S.C, Fabriol, H., 2004 – Passive Seismic Imaging of CO_2 Sequestration at Weyburn, SEG Int'l Exposition and 74th Annual Meeting

Miranda, R., Valadares, V., Terrinha, P., Mata, J., Azevedo, M. D. R., Gaspar, M., Kullberg, J. C. & Ribeiro, C., 2009 – Age Constrains on the Late Cretaceous Alkaline Magmatism on the West Iberian Margin. Cretaceous Research, 30, p. 575-586

Murillas, J., Mougenot, D., Boulot, G., Comas, M.C., Banda, E., and Mauffret, A., 1990 – Structure and evolution of the Galicia Interior Basin (Atlantic western Iberian continental margin). Tectonophysics, 184, p. 297-319

Oliveira, J.T., Pereira, E., Ramalho, M., Antunes, M.T., Monteiro, J.H. (coords.), 1992 – Carta Geológica de Portugal, escala 1:500 000, Lisboa, Serviços Geológicos de Portugal

Oliveira, K. M. L., de Castro, D. L., Branco, R. M. G. C., de Oliveira, D. C., Alvite, E. N., Jucá, C. C., & Branco, J. L. C. (2018). Architectural framework of the NW border of the onshore Potiguar Basin (NE Brazil): An aeromagnetic and gravity based approach. Journal of South American Earth Sciences, 88, 700-714.

Palain, C., 1976 – Une série détritique terrígene, les "Grés de Silves": Trias et Lias inférieur du Portugal. Mem. Serv. Geol. Portugal. N.S., Lisboa, 25, 377 p.

Pena dos Reis, R., 2000 – Morfologias de talude instável em contexto de rifting. Exemplo do Jurássico superior da Bacia Lusitânica. Ciências da Terra (UNL), 5, p. 65–68

Pereira, P., Ribeiro, C., Carneiro, J., 2022 – Identification and characterization of geological formations with CO2 storage potential in Portugal, Petroleum Geoscience

Pereira, R., Rosas, F., Mata, J., Represas, P., Escada, C., and Silva, B., 2020 – Interplay of tectonics and magmatism during post-rift inversion on the central West Iberian Margin (Estremadura Spur). Basin Research, vol. 33-2, p. 1497-1519

Pinheiro, L.M., Wilson, R.C.L., Reis, R.P., Whitmarsh, R.B. & Ribeiro, A., 1996 – The western Iberian margin: A geophysical and geological overview. Proceedings of the Ocean Drilling Program Scientific Results, 149, p. 3-23

Rasmussen, E. S., Lomholt, S., Andersen, C. & Vejbæk, O. V., 1998 – Aspects of the structural evolution of the Lusitanian Basin in Portugal and the shelf and slope area offshore Portugal. Tectonophysics, Elsevier 300, p. 199-225

The PilotSTRATEGY project has received funding from the European Union's Horizon 2020 research and innovation programme under grant agreement No. 101022664

Reid, A. B., Allsop, J. M., Granser, H., Millett, A. T., & Somerton, I. W., 1990 – Magnetic interpretation in three dimensions using Euler deconvolution. Geophysics, 55(1), 80-91.

Reid, A. B., Ebbing, J., & Webb, S. J., 2014 – Avoidable Euler Errors–the use and abuse of Euler deconvolution applied to potential fields. Geophysical Prospecting, 62(5), 1162-1168.

Rey, J., Dinis, L., Callapez, P., and Cunha, P.P., 2006 – Da rotura continental à margem passiva, Composição e evolução do Cretácico de Portugal. Cadernos de Geologia de Portugal, Inst. Geol. e Mineiro – INETI, 75 p.

Ribeiro, A., Kullberg, M. C., Kullberg, J. C., Manuppella, G., & Philipps, S., 1990 – A review of Alpine tectonics in Portugal: Foreland detachment in basement and cover rocks. Tectonophysics, 184, p. 357-366

Roest, W. R., Verhoef, J., & Pilkington, M., 1992 – Magnetic interpretation using the 3-D analytic signal. Geophysics, 57(1), 116-125.

Soares, A.F., Kullberg, J.F., Bordalo da Rocha, R. & Callapez, P.M., 2012 – Tectono-sedimentary model for the evolution of the Silves Group (Triassic, Lusitanian basin, Portugal). Bull. Soc. géol. France, t. 183, no 3, pp. 203-216.

Soares, D.M., Alves, T.M., and Terrinha, P., 2012 – The breakup sequence and associated lithospheric breakup surface: Their significance in the context of rifted continental margins (West Iberia and Newfoundland margins, North Atlantic). Earth and Planet. Sci. Lett., 355-356, p. 311-326.

Stapel, G., Cloetingh, S., and Pronk, B., 1996 – Quantitative subsidence analysis of the Mesozoic evolution of the Lusitanian Basin (western Iberian margin). Tectonophysics, 266 (1–4), p. 493–507

Sutgerand, F., Lawrance, D., Legrand, P., Wraith, E., 2022 – Seismic monitoring for subsurface uncertainties at the Endurance CO_2 store, The Leading Edge, 41; https://doi.org/10.1190/tle41040253.1

Terrinha, P. et al. (2019)a – The Alpine Orogeny in the West and Southwest Iberia Margins. In: Quesada, C., Oliveira, J. (eds) The Geology of Iberia: A Geodynamic Approach. Regional Geology Reviews. Springer, Cham. https://doi.org/10.1007/978-3-030-11295-0_11

Terrinha, P. *et al.* (2019)b – Rifting of the Southwest and West Iberia Continental Margins. In: Quesada, C., Oliveira, J. (eds) The Geology of Iberia: A Geodynamic Approach. Regional Geology Reviews. Springer, Cham. https://doi.org/10.1007/978-3-030-11295-0_6

Wilson, R. C. L., Hiscott, R. N., Willis, M. G., & Gradstein, F. M., 1989 – The Lusitanian basin of west-central Portugal: Mesozoic and Tertiary tectonic, stratigraphy, and subsidence history. In Extensional Tectonics and Stratigraphy of the North Atlantic Margins, edited by A. J. Tankard and H. R. Balkwill, AAPG Mem., 40, p. 341 – 361

Witt, W.G., 1977 – Stratigraphy of the Lusitanian Basin: Shell Prospex Portuguesa (unpublished report), 61 p.

Zbyszewski, G., 1959 – Étude structurale de la vallée typhonique de Caldas da Rainha (Portugal). Mem. Serv. Geol. Portugal, 3, Lisboa, 184 p.

The PilotSTRATEGY project has received funding from the European Union's Horizon 2020 research and innovation programme under grant agreement No. 101022664

Zhao, C., Zheng, Y., Wang, Y., Zhao, L., 2022 – Seismic ambient noise auto-correlation imaging in a CO_2 storage area, Journal of Geophysics and Engineering, 19, 1134–1148

The PilotSTRATEGY project has received funding from the European Union's Horizon 2020 research and innovation programme under grant agreement No. 101022664